Aus der Klinik für Neurologie

der Medizinischen Fakultät Charité – Universitätsmedizin Berlin

DISSERTATION

"Strategies for early detection and therapy in mouse models of Alzheimer's disease and CADASIL: a correlation of histopathology, behavioral assays and biomechanics"

–

„Strategien zur Früherkennung und Therapie in Mausmodellen von Morbus Alzheimer und CADASIL: eine Korrelation von Histopathologie, Verhaltensanalysen und Biomechanik"

zur Erlangung des akademischen Grades

Doctor of Philosophy (PhD)

vorgelegt der Medizinischen Fakultät

Charité – Universitätsmedizin Berlin

von

Anna Pfeffer

aus Suhl

Datum der Promotion: 06.03.2020

Table of contents

List of abbreviations

AD	Alzheimer's Disease	**μm**	micrometer
Aß	Amyloid beta	**NaCl**	Sodium chloride
APP23	Alzheimer's disease mouse model	**NeuN**	Neuronal nuclei
BPSD	Behavioral and Psychological Symptoms of Dementia	**NiCl**	Nickelchloride
		PBS	Phosphate-buffered saline
BrdU	5'-bromo-2'-deoxyuridine	**PCR**	Polymerase Chain Reaction
BW	Body weight	**PFA**	Paraformaldehyde
CADASIL	Cerebral Autosomal Dominant Arteriopathy with Subcortical Infarcts and Leukoencephalopathy	**rpm**	rounds per minute
		RR	Rotarod
		s	Second
cm	Centimeter	**SPT**	Sucrose Preference Test
DAB	3,3'-Diaminobenzidine	**STD**	Standard environment
DCX	Doublecortin	**T**	Tesla
DG	Dentate gyrus	**TbE**	Time by entries
EE	Enriched Environment	**TE**	Echo time
EZM	Elevated Zero Maze	**TgN3**^{R169C}	Transgenic mouse model overexpressing mutant Notch3
FoV	Field of view		
h	Hours		
H₂O₂	Hydrogen peroxide	**TgN3**^{WT}	Transgenic mouse model overexpressing wildtype Notch3
HCl	Hydrochloric acid		
Hz	Hertz		
i.p.	intraperitoneal	**TR**	Repetition time
m	Meter	**WT**	Wild type control
M	Mol		
Min	Minutes		
mg	Milligram		
mm	Millimeter		
MRE	Magnetic Resonance Elastography		
MRI	Magnetic Resonance Imaging		
MSG	Motion Sensitizing Gradient		
mT	Millitesla		
MWM	Morris Water Maze		
ms	Millisecond		

Abstract (English)

The neurological diseases Morbus Alzheimer (AD) and Cerebral Autosomal Dominant Arteriopathy with Subcortical Infarcts and Leukoencephalopathy (CADASIL) both currently lack reliable early diagnostic methods. However, a diagnosis of the diseases before the onset of clinical symptoms is essential for timely intervention. Presymptomatic histopathologies include the deposition of amyloid ß or the degeneration of brain-supplying blood vessels and white matter (CADASIL) and lead to changes in the hippocampal tissue. A correlation of these changes with early cognitive and psychosocial symptoms and biomechanical tissue changes detectable by magnetic resonance elastography (MRE) was made here to evaluate aforementioned alterations as new early diagnostic markers. At the same time, the therapeutic effect of physical activity and a stimulating environment was investigated. In order to assess the learning and memory performance as well as behavioral and psychological symptoms of dementia, various behavioral tests were carried out in Study I using the AD mouse model APP23. These were correlated with hippocampal neuronal proliferation and survival rates. In Study II, hippocampal tissue biomechanics were assessed in APP23 using MRE and compared with histological changes in the hippocampus. Furthermore, in both studies the influence of an enriched environment (EE) as a therapeutic option was investigated. For this purpose, the animals were kept in either standard or EE cages until the analysis was performed at one of three different early disease stages. In Study III, mice with overexpressed wild type Notch3 (TgN3^{WT}) and mice with a CADASIL mutation (TgN3^{R169C}) were exposed to the above environments or a running wheel (RUN) to evaluate the influence of an enriched environment and physical activity on neurogenesis and the survival of neurons. Study I showed for the first time a correlation between early deficits in learning and memory, psychological symptoms and changes in hippocampal neurogenesis. A curative effect of EE was observed. In Study II, EE could not counteract the decrease in hippocampal cell count and viscosity, i.e. cellular cross-linking. In addition, MRE showed an early reduction in cell density as a reduction in elasticity, which however increased during the course of the disease due to the intracellular deposition of Aß. In the CADASIL model (Study III) neurogenesis was neither stimulated by RUN nor EE.

Overall, a correlation of histopathological and tissue-mechanical changes in the course of AD can be observed, which is also reflected in cognitive and psychosocial changes. EE constitutes an early treatment option but has not been shown to effectively improve histopathological alterations in CADASIL.

Abstract (German)

Die neurologischen Erkrankungen Morbus Alzheimer (AD) und Cerebrale Autosomal Dominante Arteriopathie mit Subkortikalen Infarkten und Leukoenzephalopathie (CADASIL) eint das Fehlen zuverlässiger diagnostischer Früherkennungsmethoden. Eine Diagnose der Krankheiten bereits vor dem Auftreten klinischer Symptome ist jedoch essentiell für eine rechtzeitige Intervention. Präsymptomale Histopathologien beinhalten die Ablagerung von Amyloid ß bzw. eine Degeneration der hirnversorgenden Gefäße und der weißen Substanz (CADASIL) und führen zu Veränderungen des hippocampalen Gewebes. Eine Korrelation dieser Veränderungen mit kognitiven und psychosozialen Frühsymptomen und biomechanischen Gewebeveränderungen mittels Magnetresonanzelastographie (MRE) wurde hier vorgenommen, um eben genannte als neue frühdiagnostische Marker zu evaluieren. Gleichzeitig wurde der therapeutische Effekt physischer Aktivität und einer reizreichen Umgebung untersucht. Zur Erfassung der Lern- und Gedächtnisleistung sowie Verhaltens- und psychischen Symptome von Demenz wurden in Studie I verschiedene Verhaltenstests im AD-Mausmodell APP23 durchgeführt. Diese wurden mit hippocampaler Neuronenproliferation und -überlebensrate korreliert. In Studie II wurde in APP23 die hippocampale Gewebebiomechanik mittels MRE erfasst und mit histologischen Veränderungen im Hippocampus abgeglichen. Weiterhin wurde in beiden Studien der Einfluss einer reizreichen Umgebung (Enriched Environment, EE) als Therapieoption untersucht. Hierfür wurden die Tiere bis zur Analyse an drei unterschiedlichen frühen Krankheitsstadien entweder in Standard- oder EE-Käfigen gehalten. In Studie III wurden Mäuse mit überexprimiertem Wildtyp Notch3 (TgN3^{WT}) und solche mit einer CADASIL-Mutation (TgN3^{R169C}) den o.g. Umgebungen oder einem Laufrad (RUN) ausgesetzt, um den Einfluss einer reizreichen Umgebung und physischer Aktivität auf die Neurogenese und das Überleben der Neuronen zu evaluieren. Studie I zeigte erstmals eine Korrelation zwischen frühzeitig auftretenden Defiziten in Lern- und Gedächtnisleistung, psychischer Symptomatik und Veränderungen der hippocampalen Neurogenese. Ein kurativer Effekt durch EE war hierbei zu beobachten. In Studie II konnte EE nicht einer Abnahme hippocampaler Zellzahl und Viskosität, d.h. sinkender zellulärer Vernetzung, entgegenwirken. Zudem zeigte sich in der MRE eine frühzeitig verringerte Zelldichte als Reduktion der Elastizität, welche jedoch im Rahmen der intrazellulären Ablagerung von Aß im Krankheitsverlauf anstieg. Im CADASIL Modell (Studie III) blieb eine Stimulation der Neurogenese durch RUN und EE aus.

Insgesamt ist eine Korrelation von histopathologischen und gewebemechanischen Veränderungen im Krankheitsverlauf von AD festzustellen, welcher sich auch in kognitiven

und psychosozialen Veränderungen widerspiegelt. EE stellt hierbei eine frühzeitige Therapieoption dar, die allerdings im Rahmen von CADASIL die histopathologischen Veränderungen nicht positiv beeinflussen konnte.

1 Introduction

Although Alzheimer's disease (AD) is one of the most common types of dementia and subject to a great variety of studies, reliable early diagnostic tools or lasting effective therapies are not yet available. These challenges also concern other neurodegenerative diseases including the less common Cerebral Autosomal Dominant Arteriopathy with Subcortical Infarcts and Leukoencephalopathy (CADASIL). CADASIL is the most prevalent genetically hereditary disease to cause strokes and thereby later dementia[1]. The cognitive decline observed in both diseases[1, 2] reflects underlying histopathological changes in the brain. In CADASIL, arterial accumulations of granular osmiophilic extracellular material caused by a mutation in the Notch3 gene lead to a progressive degeneration of vascular smooth muscle cells and in consequence to arterial dysfunction. The associated inadequate or even disrupted blood supply results in white matter infarcts[3]. These are mainly considered causal for the cognitive decline associated with the disease[4] and characterized by an early, progressing dementia including memory loss, deficits in executive function and verbal fluency as well as apathy and a narrowed field of interest[5]. However, such deficits are observed also before infarcts[6] and possibly associated with the presence of Notch3 in neuronal precursor cells of the hippocampus[7], an area crucial for memory and learning processes. In AD, the presence of Amyloid beta (Aß) plaques is associated with disturbed neurogenesis, inflammation processes and neurodegeneration particularly in the hippocampus[8]. Besides impaired learning and memory, symptoms that arise with the occurrence of plaques also include Behavioral and Psychological Symptoms of Dementia (BPSD)[2, 9]. At present, AD is only diagnosed when these outward symptoms are detected. At that timepoint, neuropathological processes have already damaged the brain[10]. Available therapies may lead to a temporary improvement but cannot avert the fatal outcome of the disease. An early diagnosis is therefore crucial to start therapy in time to prevent the progression of AD. Studies of AD mouse models suggest that cognitive symptoms as well as BPSD already occur in the pre-plaque stage[11]. A correlation of such symptoms with neuronal properties of the hippocampus provides important information about the early stage of the disease and at the same time evaluates the suitability of cognitive and behavioral symptoms as pre-plaque markers for potential early neurodegenerative processes. Another approach for a non-invasive diagnosis of AD is Magnetic Resonance Elastography (MRE), which allows the measurement of tissue viscoelasticity[12]. Examinations in an AD model[13] suggest that alterations of the biomechanical properties of the brain reflect underlying pathological changes and can thus help to detect neurodegenerative disease before any symptoms occur. A social and active lifestyle, constituted in mouse models by an

enriched environment (EE), has a beneficial effect on the survival of proliferating neurons in the adult brain[14]. EE also improves cognition in both AD patients and models, which indicates that a change of lifestyle towards more social and physical activity may help prevent neurodegeneration in AD and also CADASIL.

In study I, neurogenesis and survival of newly generated neurons in the hippocampus were assessed in an AD mouse model to investigate potential disturbances of the neuronal network in the pre-plaque stage. Since these might be accompanied by cognitive symptoms and BPSD that could serve as disease indicators, parameters of cognitive and behavioral tests were related to neuronal cell analysis. At the same time, the therapeutic effect of an enriched environment on early disease progress was evaluated.

Closely linked with these ideas, MRE was tested as an early diagnostic tool for AD in study II. To correlate viscoelastic properties with disease progression, the number of neurons and presence of Aß in the hippocampus of an AD mouse model was measured in both a standard and an enriched environment.

Study III included a mouse model of CADASIL in an early disease stage. The animals were exposed to physical activity or EE to investigate their impact on neurogenesis and neuronal survival and thus therapeutic potential.

2   Methodology

2.1   Animals

All transgenic mice were bred in the Research Institute for Experimental Medicine (FEM) within Charité Universitätsmedizin Berlin. The animals were kept with *ad libitum* access to food and water in humidity- and temperature-controlled rooms at a 12h/12h light/dark cycle throughout the duration of the experiments. In all studies, only female animals were used to minimize conflicts and stress in larger animal groups. The experiments were approved by the responsible ethics committee (Landesamt für Gesundheit und Soziales, Berlin) and carried out in accordance with the "Directive 2010/63/EU of the European parliament and of the council of 22 September 2010 on the protection of animals used for scientific purposes" and the German animal welfare law. In all studies the experimenters were blinded to the experimental conditions whenever automated analysis was not possible.

2.1.1   APP23 mouse model of AD

In study I and II, mice of the transgenic strain APP23 (APP23) were used as an animal model for AD and entered the experiment aged five weeks. The animals are based on a C57Bl/6J

background and express human APP751 cDNA with the Swedish double mutation under the murine Thy- 1.2 gene[15]. PCR of ear biopsies was performed to confirm the genotype of the single animal (Primers: APP ct forward: 5' GAA TTC CGA CAT GAC TCA GG 3', APP ct reverse: 5' GTT CTG CTG CTG CAT CTT CGA CA 3'). C57Bl/6J mice (Charles River, Sulzfeld, Germany) of the same age were used as wild type control (WT).

2.1.2 TgN3^{R169C} mouse model for CADASIL

Study III included twelve-week-old animals of the transgenic lines TgN3^{R169C} and TgN3^{WT}, which both overexpress the mutant respectively the wild type Notch3 transcript. In TgN3^{R169C} animals, a R169C point mutation at the exon 4 of the *notch3* gene is responsible for typical symptoms of CADASIL. Wild type Notch3 is expressed in the TgN3^{WT} mouse[16]. PCR of ear biopsies was performed to confirm the genotype of each animal (Primers: Notch3 forward: 5' TTC AGTGGTGGCGGGCGTC 3'; Notch3 reverse: 5' GCCTACAGGTGCCACCATTA CGGC 3'; Vector forward: 5' AACAGGAAGAATCGCAACGTTAAT 3'; Vector reverse: 5' AATGCA GCGA TCAACGCCTTCTC 3'). Age-matched FVB/N mice (Janvier, Le Genest-Saint-Isle, France) served as WT.

2.2 In vivo designs

2.2.1 Study I: Behavioral and psychological symptoms of dementia (BPSD) and impaired cognition reflect unsuccessful neuronal compensation in the pre-plaque stage and serve as early markers for Alzheimer's disease in the APP23 mouse model[17]

At the age of five weeks, WT and APP23 mice were randomly assigned to standard (STD) and enriched environment (EE) cages. A STD cage is a conventional laboratory cage (Makrolon cages, 0.27 m × 0.15 m × 0.42 m) housing five animals. An EE cage (0.74 m × 0.3 m × 0.74 m) contains ten animals to provide social enrichment and various plastic tubes, boxes and houses that are reassembled on a weekly basis to constitute a diversified environment. The animals were kept in their assigned home cage until the start of the behavioral experiments (elevated zero maze, sucrose preference test, rotarod, Morris water maze) after either one (1W / adolescent), twelve (12W / young-adult) or 24 weeks (24W / adult) and also during the experimental period except for the sucrose preference test. Subsequently, at a final age of eight, 19 or 31 weeks the animals were sacrificed for further histological analysis of the brains. For that purpose, the animals were deeply anesthetized and then perfused transcardially. Four weeks (1W: three weeks) prior to perfusion, all mice

received the cell proliferation marker 5-Bromo-2′-deoxyuridine (BrdU) dissolved in 0.9% saline as an intraperitoneal (i.p.) injection every 24h during three consecutive days. A detailed timeline of the setup is provided by *Pfeffer et al. (2018)*, Fig. 1[17].

2.2.2 Study II: MR elastography detection of early viscoelastic response of the murine hippocampus to amyloid beta accumulation and neuronal cell loss due to Alzheimer's disease[18]

A random selection of ten animals from both APP23 and WT underwent an initial MRE measurement at the age of six weeks to obtain baseline data before all animals were assigned to their cages. Separation of WT and APP23 mice into STD and EE cages was carried out similarly to study I. The animals remained in their assigned cage until the MRE measurement was performed after one, twelve or 24 weeks (corresponding to adolescent, young-adult or adult). Afterwards, the animals were sacrificed as described for study I. A detailed depiction of the experimental setup can be found in *Munder et al. (2018)*, Fig. 1[18].

2.2.3 Study III: Stimulation of adult hippocampal neurogenesis by physical exercise and enriched environment is disturbed in a CADASIL mouse model[19]

Mice of the strains FVB/N (WT), TgN3^{R169C} and TgN3^{WT} were randomly assigned to STD or EE cages as described in study I, or to a conventional cage containing two animals and a running wheel (RUN) (Tecniplast, Italy). An LCD counter was used to register wheel turns and thus measure the distance covered on the wheel. The animals were kept in their assigned home cage for either 28 days (short-term) or six months (long-term). At the beginning of the experiment, each mouse received three consecutive i.p. injections of BrdU in intervals of 4 h. A further group of FVB/N (WT), TgN3^{R169C} and TgN3^{WT} was kept in STD cages for 28 days before their performance in the Rotarod was analyzed. All animals were sacrificed analogous to study I. For a graphic description of the setup and procedures, please refer to *Klein et al. (2017)*, Fig. 1[19].

2.3 Behavioral Testing
2.3.1 Elevated Zero Maze

Mice were tested in the elevated zero maze (EZM) to measure anxiety, a component of BPSD (study I). The experiments took place in the morning under consistent lightning conditions. To provoke the natural aversion of mice to open spaces and height, one animal at a time was placed on a circular maze with a 5.5 cm wide catwalk positioned 40 cm above the ground and

divided into for quadrants – two walled, closed and two open quadrants. The animal's behavior was then video recorded for 5 min and the following parameters were assessed: The time spent in the open quadrant was analyzed using Viewer³ Software (Biobserve), while entries from closed into open quadrants and head dips were counted manually. Another parameter, Time by Entries (TbE)[20], was calculated with the following formula: *TbE = (Time in Open Quadrants) / √(Number of Entries).* Head dips and time spent in the open quadrant represent anxiety and are influenced by the animals' activity level, indicated by the number of entries. Their increase indicates reduced anxious behavior[21]. In the parameter TbE, the influence of activity is eliminated. TbE and anxiety are negatively correlated.

2.3.2 Sucrose Preference Test

To test for anhedonia as a symptom of depression and BPSD[22], a sucrose preference test (SPT) was performed (study I). In rodents, anhedonia is reflected e.g. in a decreased interest for sugared water[23]. Based on this background, the mice were placed into STD cages containing two drinking bottles and housing two animals each. In an initial 12 h training phase, the animals received drinking water containing 5% sucrose for habituation. Subsequently, the mice received regular drinking water for 12 h before entering the actual test. In the test phase, both drinking water and 5% sucrose solution were provided and the amount of consumed liquids was measured after 12 h and 24 h. Food was provided *ad libitum* at all times. The sucrose preference was then calculated as follows:

$$Sucrose\ Preference\ (\%) = \frac{Sucrose\ total}{Sucrose\ total\ +\ Water\ total}\ x\ 100\ ^{24}.$$

2.3.3 Rotarod

Motor coordination was examined in study I and III using the well-established rotarod setup. In study I, mice were first trained on the rotarod apparatus (TSE Systems) in four trials on each of two consecutive days. On day three, motor coordination was tested in three trials and performance recorded automatically as latency to drop off the rod (TSE RotaRod Version 4.1.7 Software). Here, five mice per trial were placed in separate sections on the rotating rod, which was accelerated in six steps from four to 40 rounds per minute (rpm) with a total running time of five minutes (Phase 1: 10 s, 4 to 10 rpm; Phase 2: 50 s, 10 rpm; Phase 3: 60 s, 10 to 20 rpm; Phase 4: 60 s, 20 to 30 rpm; Phase 5: 60 s, 30 to 40 rpm; Phase 6: 60 s, 40 rpm). The mice were able to recover during an inter-trial interval of 30 min. In study III, mice were tested in three consecutive trials on one day. The speed of the Rotarod (Columbus instruments, Columbus, OH, USA) was accelerated continuously from 5 to 65 rpm.

2.3.4　Morris Water Maze

Visuo-spatial memory and the ability of hippocampus-dependent (flexible) learning was assessed in the Morris Water Maze (MWM) (study I). On five consecutive days in six trials each, mice were tested in a circular pool (diameter: 1.2 m) filled with opaque water (19 ± 1 °C) and containing a hidden platform 1 cm under the surface. With geometrical cues providing orientation, the animals were supposed to find the hidden platform within a period of 2 min based on an established protocol[25]. After the acquisition phase (day 1 to 3), the hidden platform was relocated to analyze reversal learning abilities (day 4 to 5, reversal learning phase). The starting point changed daily. A detailed visual description of starting points and platform positions can be found in *A. Pfeffer et al. (2018)*, Fig. 4[17]. Mice were directed to the platform and kept there for five seconds to memorize the position in case they did not find the goal within the trial period. The animals were able to recover after each trial for at least 30 min. All trials were recorded, tracked and analyzed using Viewer³ Software (Biobserve). The parameters average velocity and latency were used to calculate the covered distance to the target, and the time spent in the previous target quadrant.

The xy-coordinates of the prevailing spatial position in each trial were transformed into a heatmap image by using an established algorithm[25] for MATLAB (Mathworks, USA). This also allowed a qualitative analysis of search strategies and thus learning abilities. As previously described[25], strategies are categorized into hippocampus-dependent "spatial" and -independent "non-spatial" strategies as well as "perseverance". The latter describes a behavior on the first trial of the reversal learning phase characterized by abidance in the previous goal quadrant.

2.4　Magnetic Resonance Elastography

The MRE measurement in study II was conducted in a 7T MRI Scanner (Bruker Pharma Scan, Ettlingen, Germany). Throughout the whole process the mice were anesthetized with isoflurane / oxygen through a face mask, kept on a temperature-controlled heating mat and monitored via a respiration sensor. First, T_2-weighted MRI images were created to select the regions of interest – cortex and hippocampus – for the subsequent elasticity measurement. To transfer vibration generated by the electromagnetic Lorentz coil to the mouse brain, the animals were placed on a tooth bar integrated in the face mask and connected to the coil. The imaging sequence was altered for MRE by sinusoidal motion sensitizing gradient (MSG) in the through-plane direction with a strength of 285 mT/m, a frequency of 900 Hz and 9 periods. Further imaging parameters were: 128 x 128 matrix, 25 mm FoV, 14.3 ms TE, 116.2

ms TR, eight time steps over a vibration period. For each brain, four axial slices of 1 mm thickness were produced. To visualize elasticity as wave images, a 2D-Helmholtz inversion was conducted, producing the complex shear modulus G*. Tissue elasticity, which is mainly influenced by different cell types, is represented in the real part of G*, $G' = Re(G^*)$. The imaginary part of G*, $G'' = Im(G^*)$, gives information about tissue viscosity, which is determined by the density and three-dimensional structure of the cellular network. A close description of the setup and imaging process is provided in *Munder et al. (2018)*[18].

2.5   Perfusion and tissue processing

At the end of all experiments, brain tissue was collected. For this purpose, animals were deeply anaesthetized by i.p. application of Ketamine / Xylazine. Subsequently, a transcardial perfusion was carried out first with phosphate-buffered saline (PBS) and then paraformaldehyde (PFA). Brains were removed and stored in PFA for 24 h (4 °C) before being transferred into 30 % sucrose solution (4 °C, 48 h) for dehydration. The tissue was then frozen in 2-methylbutane in liquid nitrogen at -70 °C and stored until histological analysis at -80 °C. For histological staining brains were cut into 40 μm thick slices and stored at 4 °C in 24-well-plates in cryoprotectant solution.

2.6   Histology and cell quantification

2.6.1   Immunohistochemistry

To detect and quantify the number of proliferating cells (study I and III), microglia and macrophages (study I), and intracellular Aβ (study II), series of free-floating brain sections were stained against the respective markers BrdU (proliferating cells; study I/III; one-in-six series), Iba-1 (microglia, macrophages; study I; one-in-six series), or 4G8 (Aβ; study II; one-in-twelve series). After pre-treatment with H_2O_2 (and HCl in case of BrdU) and blocking with PBS+ (0.1 % Triton, 3 % donkey serum), the tissue was incubated overnight with a diluted primary antibody. Subsequently, the slices were exposed to a diluted biotinylated secondary antibody and then a streptavidin peroxidase complex (Vectastain). The binding of antibodies was visualized by 3,3'-Diamoniobenzidine (DAB)-NiCl staining before the brain slices were mounted onto object slides and coverslipped.

2.6.2   Immunofluorescence

To determine the proliferation stage of neuronal cells in study I and neuronal and astrocytic cell types in study III, a one-in-six series of free-floating brain sections was triple stained

against BrdU, Doublecortin (DCX) and Neuronal Nuclei (NeuN) (study I), or BrdU, NeuN and S100ß (study III). Briefly, sections were treated with HCl, blocked with PBS+ and then incubated over night with the diluted primary antibodies. The following day, the sections were exposed to the diluted secondary antibodies Rhodamine X, Alexa 647 and Alexa 488 before being mounted onto object slides and coverslipped.

2.6.3 Histological staining

To detect Aß plaques in APP23 (study I and II), a one-in-twelve series of brain sections of representative animals for each group was washed in PBS and mounted onto object slides. Once dried, the sections were incubated in matured haemalaun and afterwards washed under running tap water. Subsequently, the tissue was exposed to a solution of saturated alcoholic sodium chloride (2% NaCl in 80% ethanol, 1% aqueous NaOH per 100 ml) and afterwards in a solution of saturated alcoholic sodium chloride and Congo red. In a final step, the slides were washed, dehydrated and coverslipped.

To quantify the number of cells in the cortex and hippocampus (study II), cell nuclei were labelled with the DNA-binding fluorochrome 4′6-diamidino-2-phenylindole (DAPI). For this purpose, free-floating one-in-twelve series of brain sections were washed before being incubated with DAPI diluted in PBS. After a final washing step, the brain sections were mounted onto object slides and coverslipped.

2.6.4 Cell quantification

To quantify proliferating cells, the number of BrdU-positive (BrdU+) cells in the dentate gyrus (DG) including the subgranular zone and granule cell layer was counted using a light microscope (Zeiss Axioskop) with a 40x objective. Of each animal, seven (study I) or nine (study III) tissue sections were analyzed. The number of BrdU+ cells was multiplied by six to estimate the total number of proliferating cells in the DG.

Pictures of Iba-1-labelled cells in four sections per animal were taken with a Leica Dmi8 microscope (study I). In three animals per group, the number of Iba-1-positive (Iba-1+) cells was counted manually in the left and right DG using the Cell Counter Plug-In of Image J (NIH, USA). The number of Iba-1+ cells was multiplied by six to extrapolate the amount of microglia and macrophages to the whole DG.

4G8-positive (Aß+) cells were counted in the cortex and hippocampus of the left and right hemisphere of five animals per APP23 group (study II). WT were not analyzed as they show no immunoreactivity to 4G8. Using a Leica DMRE microscope equipped with

StereoInvestigator (MicroBrightfield) software, the brain areas were defined under a 5x objective based on the mouse brain atlas (Bregma -0.58 to -4.49 mm). With the software randomly providing counting frames (60 μm x 60 μm x 60 μm; sampling grid 500 μm x 500 μm over the region of interest (ROI); Optical Dissector height 20 μm, starting 5 μm below top surface), plaques were counted in one-in-twelve sections under a 100x oil objective. Based on the pre-settings described above and the number of manually counted cells, the cell numbers of the selected brain regions were counted automatically.

The same procedure, settings and microscope were used to quantify DAPI-labelled (DAPI+) cells in study II. Here, the cortex of three and hippocampus of five mice per group were analyzed in one of six tissue sections per mouse.

The quality of proliferating cells in study I was examined with a confocal microscope (Leica TCS SP2) under a 40x oil objective. For each animal, 50 BrdU+ positive cells in the granule layer of the respective brain sections were selected randomly. By taking z-stacks, the co-expression of BrdU/DCX-positive (BrdU+/DCX+, neuronal precursor cells) and BrdU/NeuN-positive (BrdU+/NeuN+ mature granule cells) was visualized. To extrapolate the absolute number of the specific cell types, the total number of BrdU+ cells was multiplied by the ratio of BrdU+/DCX+ and BrdU+/NeuN+ cells obtained from the 50 analyzed fluorescently marked cells. Proceedings in study III to investigate the co-labeling of BrdU+/NeuN+ and BrdU/S100ß-positive cells (BrdU+/S100ß+, astrocytic cells) in the rostrocaudal extent of the DG were similar. Here, a Leica DM 2500 microscope was used.

The extracellular plaques labelled with Congo red in study I and II were detected and counted manually using a light microscope (Olympus BX60 – study I; Zeiss Axioskop – study II).

2.7 Statistical Analysis

Statistical analysis was performed using IBM SPSS Statistics (Armond, NY. Version 19: study II; version 23: study I/III) and graphic presentation was realized with Graph Pad Prism (San Diego, CA. Version 5: study II/III; version 7: study I). The level of significance was set to $P \leq 0.05$.

In study I and II, a three-way analysis of variance (ANOVA) was applied with the factors genotype (g; WT vs. APP23), cage (c; STD vs. EE) and duration (d; 1 week vs. 12 weeks vs. 24 weeks, respectively adolescent vs. young-adult vs. adult) for neuronal cell and microglia analysis, the EZM, rotarod and parameters of the MWM (single day distances and search strategies, perseverance and time spent in the previous target quadrant). A Bonferroni post-hoc test for pairwise comparisons was done in case of any interaction of the factors.

Furthermore, in study I, Repeated Measures ANOVA was applied to compare distances and search strategies between the test days (t; time) in the MWM and percentage amounts of consumed liquids in the sucrose preference test. The effect size for each comparison was reported as Partial Eta Squared ($η^2p$). Levene's test was performed to analyze variance homogeneity and Shapiro Wilk test was used to test for normality.

In study II, in addition, a two-way ANOVA with the factors c and d was applied to analyze data referring to cells positive for Aß in APP23 animals.

A two-way ANOVA was also performed in study III to study the effects of genotype and cage as well as their interaction on total numbers and percentages of proliferating, mature granule and astrocytic cells. One-way ANOVA served to analyze Rotarod performance and running wheel activity in the short- and long-term group. In case of significant interaction of the factors, pairwise comparisons were done using the Bonferroni post-hoc test.

Table 1: List of all substances used in the experiments and analysis including dilution and dose applied.

Substance	Abbreviation	Dilution/Dose	Company
2-Methylbutane			Merck
3,3'-Diaminobenzidine	DAB	0.025 mg/ml	Sigma-Aldrich
4G8 mouse-antibody (Aß$_{17-24}$ antibody)	4G8	1:1000	BioLegend
4′6-diamidino-2-phenylindole	DAPI	1:1000	Thermo Scientific
5'-Bromo-2'-deoxyuridine	BrdU	10 mg/ml, 50 mg/kg BW	Sigma-Aldrich
5'-Bromo-2'-deoxyuridine antibody rat		1:500	Biozol (study I) AbD serotec (study III)
Alexa 488 mouse, rabbit		1:1000	Invitrogen
Alexa 647 mouse		1:300	Dianova
Alexa 647 goat		1:300	Invitrogen
Biotin rat, rabbit		1:250	Dianova
Congo red			Sigma-Aldrich
Donkey Serum		3ml / 100ml PBS	EMD Millipore Corp
Doublecortin antibody goat		1:100	Santa-Cruz
Ethanol		800ml/l	Roth
Haemalaun			Merck
Hydrochloric acid	HCl	2 M	Merck
Hydrogen peroxide 30%	H$_2$O$_2$	20 ml/l	Roth
Ionized calcium-binding adaptor molecule 1 antibody rabbit		1:1000	Wako
Isoflurane		1.5 - 4% (O2: 0,3%/l air)	CP Pharma
Ketamine hydrochloride 10%	Ketamine	0.75 ml/25 g BW	WDT
Neuronal nuclei antibody mouse		1:1000	Millipore
Nickelchloride	NiCl	0.4 mg/ml	Sigma-Aldrich
Paraformaldehyde	PFA	40 g/l	Sigma-Aldrich
Phosphate-buffered saline	PBS	pH = 7.4, 0.1M	Roth
Rhodamine X rat		1:250	Dianova
S100ß antibody rabbit		1:150	Abcam
Sodium chloride	NaCl	20ml/l	Roth
Sodium hydroxide	NaOH	1mg/100ml	Roth
Sucrose Solution		5 g/l	Roth
Sucrose Solution		30 g/l	Roth
Triton X-100 10%	Triton	10 ml/l	Fluka
Vectastain® ABC Elite kit	ABC reagent	9 µl/ml	Vector Laboratories
Xylazine (Rompun) 2%	Xylazine	0.25 ml/25 g BW	Provet AG

3 Results

3.1 Study I: Reduced anxiety behavior and early deficits in visuo-spatial memory and learning flexibility are accompanied by impaired neuronal maturation, all partly reversible by exposure to EE

In the EZM, APP23 spent more time in the open quadrants compared to WT (*P < 0.001*). This reduction in anxiety was also present under EE condition at all ages (*WT vs. APP23 1W: P = 0.009; 12W / 24W: P < 0.001*). At the same time, the activity level represented by the number of entries into the open quadrant was significantly higher in APP23 under both cage conditions (*WT vs. APP23 STD: P = 0.004; EE: P < 0.001*). The number of entries performed by APP23 in STD decreased with duration (*APP23 STD 1W vs. 12W: P < 0.001; 1W vs. 24W: P = 0.004*). The reduction of the parameter TbE in APP23 compared to WT (*WT vs. APP23: P < 0.001*) indicates a decrease of mere anxiety in the transgenic mice.

The SPT, in which all experimental groups preferred sucrose solution to water (*P < 0.001*), and the RR test (*genotype x duration x condition: P = 0.322*) revealed no differences between WT and APP23.

Analysis of covered distances in the MWM showed a significantly inferior performance of APP23 compared to WT throughout the acquisition phase, both in STD (*WT vs. APP23: P = 0.001*) and EE (*WT vs. APP23: P < 0.001*). However, adolescent and young-adult animals were able to improve their performance on day 3 to a distance similar to WT (*WT vs. APP23 1 W: P=0.021; 12 W: P=0.114; 24 W: P=0.001*). On the first day of the reversal learning phase (day 4), all animals covered significantly longer distances compared to day 3 (*day 3 vs. 4: P < 0.001*). Measurement of the perseverance and time spent in the previous target quadrant in the first trial of day 4 shows that both genotypes learned the primary platform position equally well (*perseverance: WT vs. APP23: P = 0.647*). However, APP23 covered longer distances in this trial (*APP23 vs. WT STD: P=0.01; EE: P = 0.048*). On day 5, APP23 swam significantly longer distances to the platform than WT (*WT vs. APP23: P < 0.001*), which improved their performance from day 4 to 5 both under the STD and EE condition. APP23 could improve their performance between these days only in the young-adult EE group (*APP23 12W EE, day 4 vs. 5: P = 0.001*), for 24W EE a trend towards decrease of distance was detectable (*APP23 24W EE, day 4 vs. 5: P=0.056*).

Regarding the search strategies applied in the MWM, APP23 were less likely to use spatial strategies than WT in STD (*WT vs. APP23: P = 0.007*). In contrast to covered distances, EE did not only have a positive effect on WT, but also increased the use of spatial strategies in APP23 (*STD vs. EE WT: P=0.003; APP23: P=0.015*).

Congo red staining confirmed the APP23 model as Aß plaques appeared only from 24W in both STD and EE transgenic mice and not in WT. Characterization of neuronal cell types revealed a significantly higher prevalence of neuronal precursor cells (BrdU+ / DCX+) in 1W STD APP23 compared to the age-matched WT (*1W STD WT vs. APP23: P = 0.011*). This effect was even stronger in EE (*1W EE WT vs. APP23: P < 0.001*) but diminished with age in both cage conditions and genotypes. The number of mature neurons (BrdU+ / NeuN+) was similar for all groups in STD. Exposure to EE had a positive effect on WT until young-adulthood (*WT STD vs. EE 1W: P < 0.001; 12W: P=0.063; 24W: P=0.238*). In APP23 a similar effect could be observed in young-adult animals (*APP23 12W STD vs. EE: P < 0.001*) and significantly more mature neurons were detected than in the corresponding WT (*APP23 vs. WT 12W EE: P=0. 028*).

The analysis of Iba-1+ cells revealed a general reduction of these cells with age (*1W vs. 12 W: P=0.009; 1W vs. 24 W: P=0.003*). At the same time, the number of microglia was increased in APP23 (*WT vs. APP23: P=0.002*) and especially in EE condition (*APP23 24 W STD vs. EE: P < 0.001*). For enhanced readability, F-values have been omitted in this paragraph and can be found in the supplementary table to *Pfeffer et al. (2018)*[17] on pages 50 ff.

3.2 Study II: Changes on the cellular level involve alteration of hippocampal visoelastic properties and histopathologic signs of AD

MRE measurements of the hippocampus revealed a reduced viscosity in APP23 compared to WT (*F(1,82) = 8.469, P = 0.005*), especially prominent in adult animals (*F(2,78) = 7.222, P = 0.001; 24 W WT vs. APP23: P < 0.001*). The exposure to EE resulted in increased viscosity in WT (*F(1,80) = 4.798, P = 0.007*), but no effect of EE could be observed in APP23 (*P = 0.838*).

Also in the hippocampus, the number of DAPI+ cells generally decreased with age (F(2,58) = 21.688, P < 0.001; 1W vs. 12W vs. 24W: P < 0.001). At the same time, the amount of DAPI+ cells in adult and adolescent APP23 kept in STD condition was lower than in age-matched WT (*F(2,55) = 4.575, P = 0.015; WT vs. APP23 12W: P = 0.001, 24W: P < 0.001*). However, in the AD model more DAPI+ cells could be detected in the hippocampus under EE compared to STD condition (*F(1,57) = 26.097. P = 0.001*). This was reflected in a hippocampal cell number similar to the WT (*P = 0.989*), but the effect diminished with age (*F(2,54) = 2.822, P = 0.069; EE WT vs. APP23 1W: P = 0.002, 12W: P = 0.066, 24W: P = 0.350*). In APP23, a correlation between DAPI+ cells and viscosity (*r = 0.632, P = 0.011*)

under EE condition suggests that viscosity increases with cell density in the hippocampal tissue.

While hippocampal elasticity was not affected by age progress in WT ($F(2,81) = 3.794, P = 0.027; 1W$ vs. $12W: P = 0.684; 12W$ vs. $24W: P = 0.260$), age and elasticity were positively correlated in APP23 ($F(2,78) = 3.928, P = 0.024; 1W$ vs. $12W: P = 0.026; 1W$ vs. $24W: P = 0.003$). The analysis of Aß+ cells in the hippocampus of APP23 revealed a trend towards an age-dependence of these cells ($F(2,28) = 3.199, P = 0.059$) with a decrease from 12W to 24W ($P = 0.057$). While EE had neither impact on WT nor APP23, ($F(1,80) = 0.009, P = 0.926$), a positive correlation between cells containing Aß and elasticity could be observed in APP23 exposed to EE ($r = 0.536, P = 0.04$).

An analysis of the cortex resulted in similar viscous properties for both WT and APP23 ($F(1,83) = 0.464, P = 0.498$). Also, no effect of EE on either viscosity ($F(1,81) = 0.069, P = 0.794$) or elasticity ($F(1,81) = 0.326, P = 0.570$) could be observed for either genotype. However, duration had an effect on cortical tissue: with age, the number of DAPI+ cells decreased ($F(2,33) = 0.464, P = 0.002; 1W$ vs. $24W: P = 0.008$), while the amount of Aß+ cells in APP23 increased with age ($F(2,30) = 3.660, P = 0.041; 1W$ vs.$12W: P = 0.037$). A trend towards an increase with duration could also be observed for elasticity ($F(2,82) = 3.242, P = 0.045; 12W$ vs. $24W: P = 0.063$). Results are visualized in *Munder et al. (2018)* [19], figures 3 to 5.

3.3 Study III: While neurogenesis is unaltered in Notch3 overexpressing and CADASIL mice under short-term condition, exposure to RUN and EE fails to stimulate neurogenesis in both age groups

Under the STD long-term condition, TgN3[WT] showed a reduced amount of BrdU+/NeuN+ cells compared to WT and CADASIL ($F(4,53) = 2.415, P = 0.06;$ TgN3[WT] vs. WT: $P < 0.01;$ TgN3[WT] vs. TgN3[R169C]: $P < 0.05$). Thus, the overexpression of Notch3 reduces the survival of newborn neurons within a period of six months.

In the long-term group the number of BrdU+/S100ß+ cells remained unaltered in TgN3[WT]. However, in CADASIL the percentage of BrdU+ cells differentiating into astrocytes was increased ($F(2,59) = 4.030, P < 0.05;$ TgN3[R169C] vs. WT: $P < 0.05$), indicating a positive correlation between astrogliosis and age. No effect of genotype on BrdU+/NeuN+ and BrdU+/Aß+ cells was observed in the short-term groups ($F(1,66) = 1.264, P > 0.05$).

The exposure to EE and RUN for 28 days stimulated the proliferation of BrdU+/S100ß+ ($F(4,60) = 6.037, P < 0.001;$ STD vs. RUN: $P < 0.001$) and BrdU+/NeuN+ cells ($F(4,60) =$

4.147, P < 0.01; STD vs. RUN and EE: P < 0.001) in WT. This effect was absent in CADASIL and TgN3^{WT} in the short-term group as well as all transgenic and WT mice in the long-term group.

Although an effect of RUN on cell proliferation could only be observed in WT, performance on the running wheel differed between genotypes. In the short-term group, compared to WT, daily activity on the running wheel was increased in TgN3^{WT} (*F(2,543) = 84.66, P < 0.001*) and decreased in TgN3^{R169C} (*P < 0.001*). Also, during the first five days of RUN condition, TgN3^{R169C} showed significantly reduced daily running activity compared to WT and TgN3^{WT} (*F(2,92) = 22.34, P < 0.001*). Over a period of six months, running distances decreased with age for CADASIL mice (*F(5,8) = 8.121, P < 0.01*) and were overall reduced in TgN3^{WT} (*F(2,1569 = 229.7, P < 0.001; TgN3^{WT} and TgN3^{R169C} vs. WT: P < 0.001*).

The latency to drop off the RR was reduced in both transgenic lines compared to WT (*F(2,16) = 6.309, P <0.001*), indicating motor deficits. A graphical presentation of the results is provided in *Klein et al. (2017)* [19], figures 2 to 5.

4   Discussion

4.1   Study I: BPSD and impaired cognition involve deficient neuronal compensation in the pre-plaque stage and serve as early markers for AD

Compared to WT, the investigation of anxiety revealed a reduced anxious behavior prior to plaque deposition in APP23, which was reflected in an increased time spent in the open quadrants and also included a rise in activity (increased entries into the open quadrants). Both time spent in and entries into the open quadrants are influenced by activity[20]. To evaluate anxiety unbiased by activity, the parameter Time by Entries (TbE)[20] was calculated for all animals. TbE in APP23 was increased compared to WT, which suggests that the level of mere anxiety in the Alzheimer model prior to plaque deposition is in fact decreased and not only a result of increased hyperactivity. These observations in the pre-plaque stadium are consistent with those derived from other AD models[26, 27]. They may be similar to agitated behavior observed in patients affected by AD[28] and can thus be an early indicator of the disease. As expected from the outcome of a previous study in AD animals[29], the exposure of APP23 to a stimulating environment resulted in further reduction of anxiety and increase of activity in mice aged 19 weeks or older. Indeed, EE not only increases the activity of different mouse strains but has also proven to enhance hippocampal neurogenesis[14]. This suggests a therapeutic benefit of EE also for human AD patients in terms of reducing anxiety as a symptom of BPSD and increasing the cognitive reserve. According to Then et al. (2013), in

animal studies "(a) the confrontation with new stimuli, (b) a high number of objects that stimulate the use of higher cognitive skills, and (c) the opportunity for the individual to carry out tasks independently" are the basic principles of EE that should also be followed when translating EE to humans[30]. These prerequisites can be met by social interaction in group activities such as board games, sports or common meals as well as personal enrichment (hobbies, music, reading, puzzles) as applied in stroke patients earlier[31].

Although depression is a common symptom of AD[32], anhedonia as one of its components could not be detected within the SPT. This result is similar to that of an earlier study by Vloeberghs et al. (2007)[33] who did not observe any signs of depression in the SPT, Tail Suspension and Forced Swim test. It is therefore likely that these behavioral assays lack the necessary sensitivity to detect all facets of depression as present in humans.

Likewise, motor impairment as observed in AD patients[34] was not reproduced in APP23 or another AD model[35]. Motoric deficits at this disease stage should therefore rather be interpreted as a sign of aging than a component of AD. However, with disease progression and expansion of the pathology to the motor cortex and subcortical areas, they can be a symptom of later AD stages.

In the MWM, APP23 showed inferior cognitive abilities compared to WT throughout the acquisition phase. However, adolescent and young-adult APP23 were able to catch up with their respective WT counterpart at the end of the acquisition phase, as did 6 to 8-week-old APP23 in another study[36]. These observations imply that although spatial memory is already impaired at an early age, it can be restored in young animals by sufficient training like repeatedly performing the MWM task. Reversal learning abilities were assessed in the second part of the MWM. On the first day of this test (day 4), both mouse strains proved to have learned the initial target position as they spent equal amounts of time in the previous target zone. Also, they covered similar distances to find the new location of the platform. But contrary to the first part of the MWM, APP23 were not able to improve their performance over time in this hippocampus-dependent reversal learning task. Particularly adult APP23 and those kept in STD swam longer distances than WT, which were able to improve their performance towards the end of the task. In addition to the described impairments, throughout the MWM, APP23 were less likely to use effective spatial search strategies than WT when exposed to STD. This unfavorable choice from a variety of well-described spatial and non-spatial strategies[25] confirms the deficiencies in spatial and reversal learning observed above.

The exposure to EE did not have any beneficial effect on APP23 in the acquisition phase but was noted in a previous study involving APP23[37]. Most likely, the positive influence of EE

does not unfold immediately but only in combination with sufficient training, which in the study above was provided by a longer acquisition phase. After three days of training, EE did also unfold its effect in the study at hand and led to improved performance of young-adult and adult APP23 in comparison to those kept under STD. In addition, the exposure to a stimulating environment improved the quality of applied search strategies in APP23 in both phases of the experiment. The pick of strategy also serves as a specifically sensitive parameter: in contrast to swimming distances measured in the MWM, it can help uncover deficienies without the necessity of sufficient prior training. Moreover, a poor choice of strategy can already be detected in adolescent APP23 when swimming distance is still unaltered.

In summary, the alterations observed in the MWM can be related to the pathological changes observed in human AD patients and the corresponding AD model[15, 38]. According to the results above, these appear long before plaques are detectable and thus constitute a valuable tool for early detection of AD. Sufficient training and exposure to EE can ameliorate these deficits in spatial learning and flexibility as therapeutic interventions in the pre-plaque stage by supporting the successful integration of newborn neurons into the hippocampal network[39].

Consistent with the deficiencies of APP23 becoming evident in the behavioral tests, histological analysis revealed alterations in neurogenesis as described below. While the proliferation pattern of neuronal precursor cells was unchanged in WT, the raised number of precursor cells in adolescent APP23 implies a compensatory mechanism to AD, which is even more prominent under exposure to EE. This compensation diminishes in young-adult animals as a result of various changes in the neurogenic niche, which include altered microvasculature[40] and the presence of inflammatory factors[41] accompanied by soluble Aß[42]. As the precursor cells generated in adolescent APP23 are only detectable as newly generated neurons in young-adult APP23, microenvironmental disturbances also seem to slow down the transformation of precursors into mature neurons. In WT, EE did not increase the number of neuronal precursor cells but of new neurons. This observation suggests that EE enhances the survival of newly generated neurons rather than the proliferation of neuronal precursors[14]. By contrast, as described above, a neurogenic reserve compensatory for AD is established in adolescent APP23. Initially a raised number of microglia, especially in APP23 STD, protects the neurogenic reserve from soluble Aß[42, 43]. However, an adequate development of precursors into functional neurons is constrained by exacerbating pathologic changes in the microenvironment. EE further increases the number of microglia present and thus improves the inflammatory response in the pre-plaque stage of AD.

Altogether, the results of this study indicate the occurrence of cognitive deficits and anxiety as a BPSD already in the pre-plaque stage of AD. A first-time correlation of these symptoms with histopathological findings indicates their close association with neurological changes in the hippocampus. Subtle behavioral and mood alterations can thus serve as early signs for the disease and provide an indication for necessary therapeutic intervention. Such intervention may be an early exposure to EE, which transferred to human patients as a socially rich and active lifestyle, can add to an effective treatment of AD by preventing or reducing cognitive decline.

4.2   Study II: Early histopathological changes in the hippocampus of APP23 are reflected in viscoelastic alterations detectable using MRE

Viscous properties in the hippocampus of APP23 were overall reduced in comparison to WT and, unlike WT, a rise in viscosity with progressing age was not detected. These results reflect the impairment of neuronal functionality during the progression of AD[8, 44]. They also imply a disturbance of modification processes that take place over time within the healthy brain[45] and involve a disintegration of the neuronal network, which eventually increases viscosity[46]. The observation that viscosity of APP23 brains remains unchanged with progressing age is coherent with the compared to WT significantly decreased number of DAPI+ cells, that is neurons.

Concerning elasticity, hippocampal values of adolescent APP23 were decreased compared to the corresponding WT, which hints at pathological alterations already present in the pre-plaque stage of AD. In general, compared to WT, elastic properties are increased in APP23 as a possible consequence of an accumulation of Aß within hippocampal neurons and later externalized Aß in the extracellular matrix. Moreover, the intracellular presence of Aß induces apoptosis of the hosting neuron[47]. This contributes to heightened elasticity as biomechanical properties of apoptotic or death cells differ from those of healthy ones[48]. The same pattern of Aß was present in the cortex of adult APP23, as expected from the onset of plaque deposition described in the literature[49]. However, other than in the hippocampus, elasticity was similar for both mouse strains and thus cannot be clearly related to cortical Aß.

The exposure to EE led to an increase of cells in the hippocampus of APP23 compared to animals of the same line kept in STD at all ages. However, cell numbers still decreased with age and disease progression under both cage conditions. As described earlier, EE has a beneficial effect on neurogenesis in the hippocampus[14], but cannot sufficiently compensate neurodegeneration induced by Aß here. The described effect of EE on cell numbers was not

reflected in hippocampal viscosity or elasticity of APP23 animals. In WT, although cell numbers were not influenced by exposure to EE, hippocampal viscosity was increased. Therefore, other factors than cells seem to additionally influence mechanical properties of the hippocampal tissue.

In summary, MRE can be evaluated as an appropriately sensitive tool to detect viscoelastic changes in the brain associated with histopathological changes characteristic for AD. In APP23, neurodegeneration is correlated with reduced hippocampal elasticity and viscosity at an early stage of the disease. However, it remains yet to be investigated whether this is a causal interrelation or whether other tissue components such as extracellular matrix, non-neuronal cells or blood supply affect viscoelasticity. Nevertheless, although EE reduces cell loss, the number of neurons decreases with disease progression as does viscosity. This implies that exposure to a socially and active environment cannot effectively prevent or hinder the alteration of tissue mechanical properties accompanying disease progression.

4.3 Study III: Notch3 overexpression causes alterations of the micromilieu that reduce the neurogenesis stimulating response to RUN and EE observed in healthy animals

The results of study III reveal in particular a reduced survival of new neurons in Notch3 overexpressing animals under STD condition in the long-term group, an effect that wasn't observed in the CADASIL model. Moreover, in contrast to an AD disease model[37], neither of the transgenic models responded positively to activity on the running wheel and environmental enrichment throughout both experimental time periods. The reduced number of mature neurons in TgN3[WT] of the long-term group is in line with previous results in six-month-old TgN3[WT], showing decreased neurogenesis already four weeks after cell labeling with BrdU[50]. This early decrease of neurogenesis therefore implies a suppression of neuronal cell proliferation due to Notch3 overexpression rather than disturbed cell survival. As shown before[51], RUN and EE had a positive effect on WT in both stimulating neurogenesis and increasing the number of astrocytic cells. These cells play a crucial role in the generation of neurons and their survival[52]. Based on these observations, the increase of astrocytic cells in CADASIL mice in the long-term group appears to be a counteraction to Notch3 overexpression and associated impaired neurogenesis.

While RUN and EE increased neurogenesis in healthy animals, these stimulants had no effect on neurogenesis in young TgN3[WT], which despite impaired motor coordination actually covered longer distances on the running wheel than WT. Thus, although the number of

neurons appears to be unchanged, Notch3 overexpression disturbs the stimulating potential of RUN and EE already in young animals. Also, in the long-term groups of both TgN3[WT] and CADASIL, running wheel activity had no positive effect on neurogenesis. Both transgenic models ran shorter distances than WT. However, the distances exceeded the daily amount required for stimulation of neurogenesis in healthy animals (> 2000 m per 24 h)[53]. Consequently, the overexpression of Notch3 impedes stimulation through physical exercise or enrichment. A downregulation of Notch3 is likely to counteract this disturbance.

In conclusion, the actual generation of neurons is neither generally affected in young Notch3 nor CADASIL animals. However, the failing response to RUN and EE stimulation in both age groups suggests a dysfunction of neurogenesis originating from non-neuronal occurrences such as microenvironmental alterations. It is likely that Notch 3 features further functions in regulating neurogenesis that might lead to changes in neurogenesis although no vascular dysfunction is observed at the same time[16].

5   Conclusion

In AD, already prior to plaque deposition, symptoms of BPSD coincide with impaired cognition, which manifests itself in defective spatial memory and flexible learning. The observed correlation of such symptoms with histological alterations suggests that histopathological processes within the neuronal network of the hippocampus may be the cause for these deficiencies but can be compensated at very early stages by increased cell proliferation. However, impeding mechanisms quickly give way to neurodegeneration and cell loss. In both AD and CADASIL, changes in the microenvironment associated with the presence of Aß and Notch3 overexpression, respectively, finally lead to neurodegeneration. A social and active lifestyle as a therapeutic approach was not successful to enhance neurogenesis in CADASIL. Possibly, the effect of EE is disguised by a strong genetic component. However, if applied sufficiently early in AD, EE can increase the neuronal reserve and hippocampal cell survival and thus alleviate the deficiencies mentioned above. MRE is sensitive to detect biomechanical tissue alterations associated with histopathological changes in AD and can thus be a useful tool for early diagnostic that may also be applicable for other neurodegenerative diseases as CADASIL.

6   Bibliography

1.   Joutel, A., et al., Notch3 mutations in CADASIL, a hereditary adult-onset condition causing stroke and dementia. Nature, 1996. 383(6602): p. 707-10.
2.   Alzheimer's, A., 2016 Alzheimer's disease facts and figures. Alzheimers Dement, 2016. 12(4): p. 459-509.
3.   Chabriat, H., et al., Cadasil. Lancet Neurol, 2009. 8(7): p. 643-53.
4.   Duering, M., et al., Strategic role of frontal white matter tracts in vascular cognitive impairment: a voxel-based lesion-symptom mapping study in CADASIL. Brain, 2011. 134(Pt 8): p. 2366-75.
5.   Rutten, J. and S.A.J. Lesnik Oberstein, Cadasil, in GeneReviews((R)), M.P. Adam, et al., Editors. 1993: Seattle (WA).
6.   Taillia, H., et al., Cognitive alterations in non-demented CADASIL patients. Cerebrovasc Dis, 1998. 8(2): p. 97-101.
7.   Irvin, D.K., et al., Expression patterns of Notch1, Notch2, and Notch3 suggest multiple functional roles for the Notch-DSL signaling system during brain development. J Comp Neurol, 2001. 436(2): p. 167-81.
8.   Selkoe, D.J., Alzheimer's disease: genes, proteins, and therapy. Physiol Rev, 2001. 81(2): p. 741-66.
9.   Shimabukuro, J., S. Awata, and H. Matsuoka, [Behavioral and psychological symptoms of dementia characteristic of mild Alzheimer patients]. Seishin Shinkeigaku Zasshi, 2008. 110(7): p. 529-35.
10.   Perrin, R.J., A.M. Fagan, and D.M. Holtzman, Multimodal techniques for diagnosis and prognosis of Alzheimer's disease. Nature, 2009. 461(7266): p. 916-22.
11.   Webster, S.J., et al., Using mice to model Alzheimer's dementia: an overview of the clinical disease and the preclinical behavioral changes in 10 mouse models. Front Genet, 2014. 5: p. 88.
12.   Riek, K., et al., Wide-range dynamic magnetic resonance elastography. J Biomech, 2011. 44(7): p. 1380-6.
13.   Murphy, M.C., et al., Magnetic resonance elastography of the brain in a mouse model of Alzheimer's disease: initial results. Magn Reson Imaging, 2012. 30(4): p. 535-9.
14.   Kempermann, G., H.G. Kuhn, and F.H. Gage, More hippocampal neurons in adult mice living in an enriched environment. Nature, 1997. 386(6624): p. 493-5.
15.   Sturchler-Pierrat, C., et al., Two amyloid precursor protein transgenic mouse models with Alzheimer disease-like pathology. Proc Natl Acad Sci U S A, 1997. 94(24): p. 13287-92.
16.   Joutel, A., et al., Cerebrovascular dysfunction and microcirculation rarefaction precede white matter lesions in a mouse genetic model of cerebral ischemic small vessel disease. J Clin Invest, 2010. 120(2): p. 433-45.
17.   Pfeffer, A., et al., Behavioral and psychological symptoms of dementia (BPSD) and impaired cognition reflect unsuccessful neuronal compensation in the pre-plaque stage and serve as early markers for Alzheimer's disease in the APP23 mouse model. Behav Brain Res, 2018. 347: p. 300-313.
18.   Munder, T., et al., MR elastography detection of early viscoelastic response of the murine hippocampus to amyloid beta accumulation and neuronal cell loss due to Alzheimer's disease. J Magn Reson Imaging, 2018. 47(1): p. 105-114.
19.   Klein, C., et al., Stimulation of adult hippocampal neurogenesis by physical exercise and enriched environment is disturbed in a CADASIL mouse model. Sci Rep, 2017. 7: p. 45372.
20.   Heredia, L., et al., Individual housing and handling procedures modify anxiety levels of Tg2576 mice assessed in the zero maze test. Physiol Behav, 2012. 107(2): p. 187-91.

21.   Braun, A.A., et al., Comparison of the elevated plus and elevated zero mazes in treated and untreated male Sprague-Dawley rats: effects of anxiolytic and anxiogenic agents. Pharmacol Biochem Behav, 2011. 97(3): p. 406-15.

22.   Snaith, R.P., Identifying depression: the significance of anhedonia. Hosp Pract (Off Ed), 1993. 28(9A): p. 55-60.

23.   Strekalova, T., et al., Stress-induced anhedonia in mice is associated with deficits in forced swimming and exploration. Neuropsychopharmacology, 2004. 29(11): p. 2007-17.

24.   Mizuki, D., et al., Antidepressant-like effect of Butea superba in mice exposed to chronic mild stress and its possible mechanism of action. J Ethnopharmacol, 2014. 156: p. 16-25.

25.   Garthe, A., J. Behr, and G. Kempermann, Adult-generated hippocampal neurons allow the flexible use of spatially precise learning strategies. PLoS One, 2009. 4(5): p. e5464.

26.   Ognibene, E., et al., Aspects of spatial memory and behavioral disinhibition in Tg2576 transgenic mice as a model of Alzheimer's disease. Behav Brain Res, 2005. 156(2): p. 225-32.

27.   Harris, J.A., et al., Many neuronal and behavioral impairments in transgenic mouse models of Alzheimer's disease are independent of caspase cleavage of the amyloid precursor protein. J Neurosci, 2010. 30(1): p. 372-81.

28.   Ballard, C. and A. Corbett, Agitation and aggression in people with Alzheimer's disease. Curr Opin Psychiatry, 2013. 26(3): p. 252-9.

29.   Pietropaolo, S., J. Feldon, and B.K. Yee, Environmental enrichment eliminates the anxiety phenotypes in a triple transgenic mouse model of Alzheimer's disease. Cogn Affect Behav Neurosci, 2014. 14(3): p. 996-1008.

30.   Then, F.S., et al., Enriched environment at work and the incidence of dementia: results of the Leipzig longitudinal study of the aged (LEILA 75+). PLoS One, 2013. 8(7): p. e70906.

31.   McDonald, M.W., et al., Is Environmental Enrichment Ready for Clinical Application in Human Post-stroke Rehabilitation? Front Behav Neurosci, 2018. 12: p. 135.

32.   Frisoni, G.B., et al., Behavioral syndromes in Alzheimer's disease: description and correlates. Dement Geriatr Cogn Disord, 1999. 10(2): p. 130-8.

33.   Vloeberghs, E., et al., Mood and male sexual behaviour in the APP23 model of Alzheimer's disease. Behav Brain Res, 2007. 180(2): p. 146-51.

34.   Buchman, A.S. and D.A. Bennett, Loss of motor function in preclinical Alzheimer's disease. Expert Rev Neurother, 2011. 11(5): p. 665-76.

35.   Lalonde, R., et al., Spatial learning, exploration, anxiety, and motor coordination in female APP23 transgenic mice with the Swedish mutation. Brain Res, 2002. 956(1): p. 36-44.

36.   Kelly, P.H., et al., Progressive age-related impairment of cognitive behavior in APP23 transgenic mice. Neurobiol Aging, 2003. 24(2): p. 365-78.

37.   Wolf, S.A., et al., Cognitive and physical activity differently modulate disease progression in the amyloid precursor protein (APP)-23 model of Alzheimer's disease. Biol Psychiatry, 2006. 60(12): p. 1314-23.

38.   Serrano-Pozo, A., et al., Neuropathological alterations in Alzheimer disease. Cold Spring Harb Perspect Med, 2011. 1(1): p. a006189.

39.   Garthe, A., I. Roeder, and G. Kempermann, Mice in an enriched environment learn more flexibly because of adult hippocampal neurogenesis. Hippocampus, 2016. 26(2): p. 261-71.

40.   Meyer, E.P., et al., Altered morphology and 3D architecture of brain vasculature in a mouse model for Alzheimer's disease. Proc Natl Acad Sci U S A, 2008. 105(9): p. 3587-92.

41.   Kielian, T., Neuroinflammation: good, bad, or indifferent? J Neurochem, 2014. 130(1): p. 1-3.

42.   Janssen, L., et al., Late age increase in soluble amyloid-beta levels in the APP23 mouse model despite steady-state levels of amyloid-beta-producing proteins. Biochim Biophys Acta, 2016. 1862(1): p. 105-12.

43. Wang, W.Y., et al., Role of pro-inflammatory cytokines released from microglia in Alzheimer's disease. Ann Transl Med, 2015. 3(10): p. 136.

44. Palop, J.J., et al., Aberrant excitatory neuronal activity and compensatory remodeling of inhibitory hippocampal circuits in mouse models of Alzheimer's disease. Neuron, 2007. 55(5): p. 697-711.

45. Nieto-Sampedro, M. and M. Nieto-Diaz, Neural plasticity: changes with age. J Neural Transm (Vienna), 2005. 112(1): p. 3-27.

46. Lu, Y.B., et al., Reactive glial cells: increased stiffness correlates with increased intermediate filament expression. FASEB J, 2011. 25(2): p. 624-31.

47. Kienlen-Campard, P., et al., Intracellular amyloid-beta 1-42, but not extracellular soluble amyloid-beta peptides, induces neuronal apoptosis. J Biol Chem, 2002. 277(18): p. 15666-70.

48. Beauquis, J., et al., Environmental enrichment prevents astroglial pathological changes in the hippocampus of APP transgenic mice, model of Alzheimer's disease. Exp Neurol, 2013. 239: p. 28-37.

49. Sturchler-Pierrat, C. and M. Staufenbiel, Pathogenic mechanisms of Alzheimer's disease analyzed in the APP23 transgenic mouse model. Ann N Y Acad Sci, 2000. 920: p. 134-9.

50. Ehret, F., et al., Mouse model of CADASIL reveals novel insights into Notch3 function in adult hippocampal neurogenesis. Neurobiol Dis, 2015. 75: p. 131-41.

51. Kempermann, G., D. Gast, and F.H. Gage, Neuroplasticity in old age: sustained fivefold induction of hippocampal neurogenesis by long-term environmental enrichment. Ann Neurol, 2002. 52(2): p. 135-43.

52. Seki, T., Microenvironmental elements supporting adult hippocampal neurogenesis. Anat Sci Int, 2003. 78(2): p. 69-78.

53. Kronenberg, G., et al., Physical exercise prevents age-related decline in precursor cell activity in the mouse dentate gyrus. Neurobiol Aging, 2006. 27(10): p. 1505-13.

Eidesstattliche Versicherung (Affidavit)

Ich, Anna Pfeffer, versichere an Eides statt durch meine eigenhändige Unterschrift, dass ich die vorgelegte Dissertation mit dem Thema: *"Strategies for early detection and therapy in mouse models of Alzheimer's disease and CADASIL: a correlation of histopathology, behavioral assays and biomechanics"* („Strategien zur Früherkennung und Therapie in Mausmodellen von Morbus Alzheimer und CADASIL: eine Korrelation von Histopathologie, Verhaltensanalysen und Biomechanik") selbstständig und ohne nicht offengelegte Hilfe Dritter verfasst und keine anderen als die angegebenen Quellen und Hilfsmittel genutzt habe. Alle Stellen, die wörtlich oder dem Sinne nach auf Publikationen oder Vorträgen anderer Autoren beruhen, sind als solche in korrekter Zitierung kenntlich gemacht. Die Abschnitte zu Methodik (insbesondere praktische Arbeiten, Laborbestimmungen, statistische Aufarbeitung) und Resultaten (insbesondere Abbildungen, Graphiken und Tabellen) werden von mir verantwortet.

Meine Anteile an etwaigen Publikationen zu dieser Dissertation entsprechen denen, die in der untenstehenden gemeinsamen Erklärung mit der Betreuerin, angegeben sind. Für sämtliche im Rahmen der Dissertation entstandenen Publikationen wurden die Richtlinien des ICMJE (International Committee of Medical Journal Editors; www.icmje.og) zur Autorenschaft eingehalten. Ich erkläre ferner, dass mir die Satzung der Charité – Universitätsmedizin Berlin zur Sicherung Guter Wissenschaftlicher Praxis bekannt ist und ich mich zur Einhaltung dieser Satzung verpflichte.

Die Bedeutung dieser eidesstattlichen Versicherung und die strafrechtlichen Folgen einer unwahren eidesstattlichen Versicherung (§156,161 des Strafgesetzbuches) sind mir bekannt und bewusst.

_____   _____

Date   Signature

Selected Publications

Anna Pfeffer had the following share in the publications listed below:

Publication I:

Pfeffer A, Munder T, Schreyer S, Klein C, Rasińska J, Winter Y, Steiner B. *Behavioral and psychological symptoms of dementia (BPSD) and impaired cognition reflect unsuccessful neuronal compensation in the pre-plaque stage and serve as early markers for Alzheimer's disease in the APP23 mouse model.* Behav Brain Res, 2018. 347: p. 300-313.

IF: 3.173 (2017)

Contribution in detail: 80%. Partly conceived and designed the study, performed experiments including animal handling, injections, behavioral experiments, brain tissue processing, and histological staining and counting, analyzed the data, wrote the manuscript and corresponded with the editor/reviewer.

Excerpt from Journal Summary list:

Journal Data Filtered By: **Selected JCR Year: 2017** Selected Editions: SCIE,SSCI

Selected Categories: **"BEHAVIORAL SCIENCES"** Selected Category Scheme: WoS

Gesamtanzahl: 51 Journale

Rank	Full Journal Title	Total Cites	Journal Impact Factor	Eigenfactor Score
14	BEHAVIOURAL BRAIN RESEARCH	25,309	3.173	0.036610

Publication II:

Munder T, **Pfeffer A**, Schreyer S, Guo J, Braun J, Sack I, Steiner B, Klein C. *MR elastography detection of early viscoelastic response of the murine hippocampus to amyloid β accumulation and neuronal cell loss due to Alzheimer's disease.* J Magn Reson Imaging, 2018. 47(1): p. 105-114.

IF: 3.612 (2017)

Contribution in detail: 10%. Partly performed animal handling, injections, brain tissue processing, histological staining and counting and revision of the manuscript.

Excerpt from Journal Summary list:

Journal Data Filtered By: **Selected JCR Year: 2017** Selected Editions: SCIE,SSCI

Selected Categories: **"RADIOLOGY, NUCLEAR MEDICINE and MEDICAL IMAGING"** Selected Category Scheme: WoS

Gesamtanzahl: 128 Journale

Rank	Full Journal Title	Total Cites	Journal Impact Factor	Eigenfactor Score
24	JOURNAL OF MAGNETIC RESONANCE IMAGING	16,398	3.612	0.027440

Publication III:

Klein C, Schreyer S, Kohrs FE, Elhamoury P, **Pfeffer A**, Munder T, Steiner B. *Stimulation of adult hippocampal neurogenesis by physical exercise and enriched environment is disturbed in a CADASIL mouse model.* Sci Rep, 2017. 7: p. 45372.

IF: 4.122 (2017)

Contribution in detail: 10%. Partly performed animal handling, brain tissue processing, histological staining and revision of the manuscript.

Excerpt from Journal Summary list:

Journal Data Filtered By: **Selected JCR Year: 2017** Selected Editions: SCIE,SSCI

Selected Categories: **"MULTIDISCIPLINARY SCIENCES"** Selected Category Scheme: WoS

Gesamtanzahl: 64 Journale

Rank	Full Journal Title	Total Cites	Journal Impact Factor	Eigenfactor Score
12	Scientific Reports	192,841	4.122	0.718960

Signature, date and stamp of the supervising University teacher

Signature of the doctoral candidate

34

Print copies of the selected publications

– Study I –

Behavioral and psychological symptoms of dementia (BPSD) and impaired cognition reflect unsuccessful neuronal compensation in the pre-plaque stage and serve as early markers for Alzheimer's disease in the APP23 mouse model.

Pfeffer A, Munder T, Schreyer S, Klein C, Rasińska J, Winter Y, Steiner B.

Behav Brain Res. 2018 Jul 16;347:300-313. Epub 2018 Mar 21.

https://doi.org/10.1016/j.bbr.2018.03.030

Study I – Supplementary Table

	Test	Interaction	F-value	Effect size (η^2_p)	Variance homogeneity – Significance (Levene's test)	Normality – Significance (Shapiro Wilk test)	
A	**EZM – Head Dips**	*c*	$F_{1,114} = 26.85$	0.21	0.178	WT	0.111
		d	$F_{2,113} = 3.62$	0.07		APP23	0.122
						1W	0.397
		g	$F_{1,114} = 1.16$	0.01		12W	0.193
						24W	0.340
						STD	0.054
						EE	0.388
	EZM – Time in Open Quadrant	*g*	$F_{1,114} = 74.17$	0.42	0.032	WT	<.001
		c x g	$F_{1,112} = 1.83$	0.02		APP23	0.792
						1W	0.282
		c x d x g	$F_{2,109} = 6.25$	0.11		12W	0.044
						24W	0.016
						STD	0.012
						EE	0.131
	EZM – Entries	*g*	$F_{1,114} = 55.76$	0.35	0.677	WT	0.003
		c x g	$F_{1,112} = 10.41$	0.09		APP23	0.282
						1W	0.135
		c x d x g	$F_{2,109} = 12.83$	0.2		12W	0.023
						24W	0.008
						STD	0.001
						EE	0.247
	EZM – Time by Entries	*c*	$F_{1,113} = 7.60$	0.07	0.020	WT	0.008
						APP23	<.001
						1W	0.498
						12W	0.002
						24W	0.120
		g	$F_{1,113} = 36.34$	0.26		STD	0.002
						EE	0.109
B	**Sucrose**	*Water vs.*	$F_{1,48} =$	0.98	< 0.001	WT	<.001

	Preference Test	*Sucrose Solution*	1920.06			APP23	0.016
						1W	<.001
						12W	0.081
						24W	0.370
						STD	0.287
						EE	<.001
C	**Rotarod**	*c*	$F_{1,113} = 1.67$	0.02	0.004	WT	0.040
		d	$F_{2,112} = 1.98$	0.04		APP23	0.527
		g	$F_{1,113} = 0.006$	< 0.001		1W	0.001
						12W	0.001
						24W	0.667
		c x d x g	$F_{2,108} = 1.15$	0.02		STD	0.187
						EE	0.115
D	**Morris Water Maze: Day 1**	*g*	$F_{1,113} = 6.19$	0.06	0,785	WT	<.001
						APP23	0.011
						1W	0.001
						12W	0.001
						24W	0.019
						STD	0.001
						EE	<.001
	Morris Water Maze: Day 1 Trial 1	*g*	$F_{1,114} = 0.54$	0.01	0.064	WT	<.001
						APP23	<.001
						1W	<.001
						12W	<.001
						24W	<.001
						STD	<.001
						EE	<.001
	Morris Water Maze: Day 2	*g*	$F_{1,113} = 6.4$	0.06	0.035	WT	<.001
						APP23	<.001
						1W	<.001
						12W	0.020
						24W	<.001
						STD	<.001
						EE	<.001

Morris Water Maze: Day 3	$d \times g$	$F_{2,109} = 8.73$	0.15	0.211	WT APP23 1W 12W 24W STD EE	0.001 <.001 0.003 <.001 <.001 <.001 <.001
Morris Water Maze: Day 4	$c \times d \times g$	$F_{2,108} = 3.102$	0.06	0.259	WT APP23 1W 12W 24W STD EE	<.001 <.001 0.003 <.001 0.001 <.001 <.001
Morris Water Maze: Day 4 Trial 1	$c \times g$	$F_{1,111} = 10.11$	0.09	0.003	WT APP23 1W 12W 24W STD EE	<.001 <.001 <.001 <.001 0.005 <.001 <.001
Morris Water Maze: Day 5	g	$F_{1,113} = 23.25$	0.18	< 0.001	WT APP23 1W 12W 24W STD EE	<.001 <.001 <.001 <.001 <.001 <.001 <.001
Morris Water Maze: Day 1 - 3	d g $c \times g$ $c \times d \times g$ t	$F_{2,112} = 8.25$ $F_{1,113} = 11.40$ $F_{1,111} = 8.16$ $F_{2,108} = 2.40$ $F_{1,114} = 25.0$	0.14 0.10 0.07 0.05 0.20	D1: 0.130 D2: 0.039 D3: 0.012	See Results Day 1/2/3	
Morris Water Maze: Day 3 - 4	t	$F_{1,114} = 50.49$	0.33	D3: 0.012 D4: 0.040	See Results Day 3/4	

	Morris Water Maze: Day 4 - 5	*g*	$F_{1,113} = 11.43$	0.10	D4: 0.040 D5: < 0.001	See Results Day 4/5	
		t	$F_{1,114} = 49.41$	0.32			
		c x d x g x t	$F_{2,103} = 3.59$	0.07			
	Morris Water Maze: Time spent in previous target quadrant, Day 4 Trial 1	*c x g*	$F_{1,111} = 6.38$	0.06	0.436	WT	0.013
						APP23	0.329
						1W	0.252
						12W	0.036
						24W	0.385
						STD	0.050
						EE	0.082
E	**Morris Water Maze: Perseverance in previous target quadrant, Day 4 Trial 1**	*g*	$F_{1,113} = 0.21$	0.002	< 0.001	WT	<.001
						APP23	<.001
						1W	<.001
		c x g	$F_{1,111} = 4.78$	0.04		12W	<.001
						24W	<.001
						STD	<.001
						EE	<.001
	Morris Water Maze: Non-spatial search strategies, Day 1 - 5	*c x g*	$F_{1,111} = 15.23$	0.13	0.984	WT	<.001
						APP23	<.001
						1W	<.001
						12W	<.001
						24W	<.001
						STD	<.001
						EE	<.001
	Morris Water Maze: Non-spatial search strategies, Day 1 - 3	*g x t*	$F_{1,114} = 5.93$	0.05	D1: 0.375 D2: 0.274 D3: 0.537	WT	<.001
						APP23	<.001
						1W	<.001
						12W	<.001
						24W	<.001
						STD	<.001
						EE	<.001
	Morris Water Maze: Non-spatial search strategies, Day 4 - 5	*c x d x g x t*	$F_{2,104} = 2.83$	0.05	D4: 0.209 D5: 0.450	WT	<.001
						APP23	<.001
						1W	<.001
						12W	<.001
						24W	<.001
						STD	<.001
						EE	<.001
	Morris	*g*	$F_{1,113} = 25.86$	0.20	0.345	WT	0.004

	Water Maze: "direct swim" vs. "directed / focal search", Day 1 - 5					APP23	<.001
						1W	<.001
						12W	0.001
						24W	0.112
						STD	<.001
						EE	<.001
F	**Number of BrdU+/DCX + cells**	d	$F_{2,109} = 114.28$	0.7	< 0.001	WT	<.001
						APP23	<.001
		$d \times g$	$F_{2,106} = 25.62$	0.34		1W	<.001
						12W	<.001
		$c \times d \times g$	$F_{2,105} = 7.16$	0.13		24W	<.001
						STD	<.001
						EE	<.001
	Number of BrdU+/NeuN + cells	$d \times g$	$F_{2,106} = 1.35$	0.26	0.008	WT	<.001
						APP23	<.001
						1W	0.082
						12W	<.001
		$c \times d \times g$	$F_{2,105} = 6.44$	0.11		24W	0.045
						STD	<.001
						EE	<.001
G	**Number of Iba-1+ cells**	c	$F_{1,34} = 7.30$	0.233	0.567	WT	0.495
		d	$F_{2,33} = 8.44$	0.413		APP23	0.365
		g	$F_{1,34} = 12.46$	0.342		1W	0.824
		$d \times g$	$F_{2,30} = 7.12$	0.372		12W	0.784
						24W	0.266
		$c \times d \times g$	$F_{2,24} = 10.16$	0.458		STD	0.174
						EE	0.993

– Study II –

MR elastography detection of early viscoelastic response of the murine hippocampus to amyloid β accumulation and neuronal cell loss due to Alzheimer's disease.

Munder T, Pfeffer A, Schreyer S, Guo J, Braun J, Sack I, Steiner B, Klein C.

– Study III –

SCIENTIFIC REPORTS

Stimulation of adult hippocampal neurogenesis by physical exercise and enriched environment is disturbed in a CADASIL mouse model

C. Klein, S. Schreyer, F. E. Kohrs, P. Elhamoury, A. Pfeffer, T. Munder & B. Steiner

In the course of CADASIL (Cerebral Autosomal Dominant Arteriopathy with Subcortical Infarcts and Leukoencephalopathy), a dysregulated adult hippocampal neurogenesis has been suggested as a potential mechanism for early cognitive decline. Previous work has shown that mice overexpressing wild type Notch3 and mice overexpressing Notch3 with a CADASIL mutation display impaired cell proliferation and survival of newly born hippocampal neurons prior to vascular abnormalities. Here, we aimed to elucidate how the long-term survival of these newly generated neurons is regulated by Notch3. Knowing that adult neurogenesis can be robustly stimulated by physical exercise and environmental enrichment, we also investigated the influence of such stimuli as potential therapeutic instruments for a dysregulated hippocampal neurogenesis in the CADASIL mouse model. Therefore, young-adult female mice were housed in standard (STD), environmentally enriched (ENR) or running wheel cages (RUN) for either 28 days or 6 months. Mice overexpressing mutated Notch3 and developing CADASIL (TgN3^{R169C}), and mice overexpressing wild type Notch3 (TgN3^{WT}) were used. We found that neurogenic stimulation by RUN and ENR is apparently impaired in both transgenic lines. The finding suggests that a disturbed neurogenic process due to Notch3-dependent micromilieu changes might be one vascular-independent mechanism contributing to cognitive decline observed in CADASIL.

Cerebral Autosomal Dominant Arteriopathy with Subcortical Infarcts and Leukoencephalopathy (CADASIL) is the most common heritable cause of stroke and vascular dementia in adults[1–3]. It represents a genetic archetype of non-hypertensive ischemic cerebral small vessel disease. CADASIL patients carry dominant mutations in the *notch3* gene, which encodes a transmembrane receptor belonging to the Notch receptor family. Notch3 is required for the structural and functional integrity of small arteries. It is predominantly expressed in vascular smooth muscle cells and pericytes, controlling their arterial differentiation and maturation[4,5]. The highly stereotyped mutations alter the number of cysteine residues in the extracellular domain of Notch3 (Notch3^{ECD}), leading to abnormal vascular accumulation of mutated Notch3^{ECD}[3]. In CADASIL, small and medium sized arteries characteristically exhibit pathognomonic deposits of granular osmiophilic material (GOM) containing mutated Notch3^{ECD}. The resulting progressive degeneration of vascular smooth muscle cells (vSMC) leads to arteriole dysfunction, followed by subcortical lacunes with white matter injury. Cortico-cortical network disruptions in the frontal lobe have also been recently reported[6]. White matter infarcts are usually considered the leading cause of the progressive decline in cognitive function[7]. However, CADASIL patients show a decline in cognitive function prior to any infarcts[8,9].

Interestingly, Notch3 has also been found to be expressed in neural precursor cells of the adult hippocampus[10]. Adult hippocampal neurogenesis is a lifelong process during which new neurons are generated in the subgranular zone (SGZ) and functionally integrated into neuronal networks[11,12]. This might represent a part of the CADASIL pathology as hippocampal neurogenesis has been demonstrated to play a crucial role in hippocampus-dependent learning and memory, maintaining cognitive flexibility during adulthood and ageing[13–15]. In general, Notch is a

Charité – University Medicine, Department of Neurology, Berlin, Germany. Correspondence and requests for materials should be addressed to B.S. (email: barbara.steiner@charite.de)
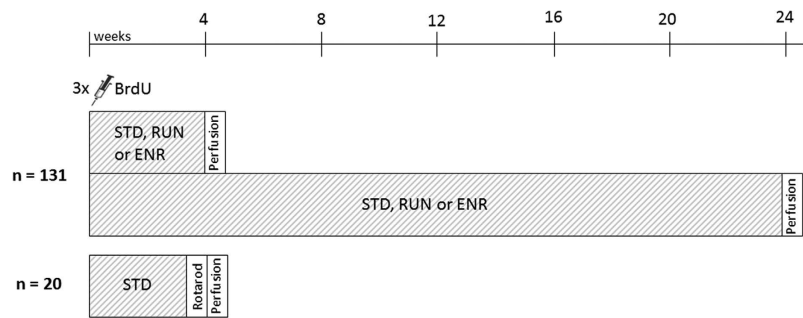
Figure 1. Experimental Design. Mice of each genotype were housed in standard (STD), running wheel (RUN) or enriched environment (ENR) cages for either a short (28 days) or a long duration (6 months).

key regulator in the crosstalk between neurogenesis and angiogenesis. It controls vessel sprouting and is required for proliferation and differentiation of stem and precursor cells[16–18]. Moreover, adult hippocampal neurogenesis occurs in a highly vascularized niche of the SGZ[19]. Here, capillaries provide the supply of nutrients and oxygen to maintain the proliferative capacity of the stem and precursor cells. As *notch3* mutations in CADASIL lead to arteriole dysfunction and decreased blood flow[20,21], it seems plausible that the resulting deficit in oxygen and glucose might influence adult hippocampal neurogenesis. Aside from the direct effect Notch3 can exert on neurogenesis by its expression in neural precursor cells, the Notch3-dependent vascular influence might, in turn, also be responsible for the observed cognitive impairments in CADASIL patients. Our previous study using a mouse model overexpressing Notch3 with a CADASIL mutation has demonstrated that adult hippocampal neurogenesis is indeed affected[22]. We have shown that neural cell proliferation and survival are reduced in the CADASIL mice at 12 months of age. This suggests functional consequences of the impaired neurogenesis on hippocampus-dependent learning and memory functions in the model and raises the question of whether physiological neurogenic stimuli might reverse the effect of the altered Notch3.

In the present study, we further elucidate how the short-term and long-term survival of newly generated neurons in the SGZ is regulated by Notch3, and how it depends on an intact Notch3 expression (Fig. 1). Adult neurogenesis can be robustly stimulated by physical exercise[23] and environmental enrichment[24]. To investigate whether a dysregulated hippocampal neurogenesis can also be improved in CADASIL by these physiological neurogenic stimuli, female adult mice were housed in standard (STD), environmentally enriched (ENR) or running wheel cages (RUN) for either 28 days (short-term) or 6 months (long-term) (Fig. 1). To address these questions, the well-established transgenic mouse model overexpressing Notch3 with a CADASIL-causing point mutation (TgN3^{R169C}) was used. To control for the effects of Notch3-overexpression in itself, mice overexpressing wild type Notch3 (TgN3^{WT}), generated by the same approach as TgN3^{R169C}, were used[25].

Results

Notch3 overexpression results in reduced survival of newborn neurons after 6 months. In the long-term group, the noticeable but non-significant interaction of genotype and cage condition revealed that TgN3^{WT} mice displayed reduced BrdU+/NeuN+ cell numbers (Fig. 2f) under STD compared to WT and CADASIL mice ($F(4,53) = 2.415$, $p = 0.06$; post-hoc: TgN3^{WT} vs. WT, $p < 0.01$, TgN3^{WT} vs. TgN3^{R169C}, $p < 0.05$). Such reduction in BrdU+/NeuN+ cell numbers under STD was not found in CADASIL mice (TgN3^{R169C} vs. WT, $p > 0.05$).

There were no changes in the number of neuronal cells in the short-term group in either transgenic mouse line under STD cage condition (WT vs. TgN3^{WT} and TgN3^{R169C}, $p > 0.05$).

Astrogliosis in CADASIL mice depends on the duration of cell survival. In the long-term group, CADASIL mice showed an increased percentage of newly generated BrdU+ cells differentiating into astrocytic S100β+ cells ($F(2,59) = 4.030$, $p < 0.05$; post-hoc: TgN3^{R169C} vs. WT, $p < 0.05$) (Fig. 3b). This was not seen in Notch3 overexpressing mice (TgN3^{WT} vs. WT, $p > 0.05$).

Astrogliosis did not occur in the short-term cell survival group in either transgenic mouse line ($F(2,66) = 1.264$, $p > 0.05$).

Representative images of the triple fluorescent staining for BrdU, S100β and NeuN are given in Fig. 4(a–h), exemplarily showing a co-labeled BrdU+/S100β+ cell (Fig. 4h) in the DG. Co-labeled BrdU+/NeuN+ cells are also presented (Fig. 4g).

Neurogenic stimulation by short-term RUN or ENR is impaired in both Notch3 overexpressing and CADASIL mice. The significant interaction of both genotype and cage condition revealed that 28 days of RUN and ENR increased the number of BrdU+ cells (Fig. 2a) only in WT mice ($F(4,60) = 4.495$, $p < 0.01$; post-hoc: STD vs. RUN and ENR, $p < 0.001$) but not in in TgN3^{WT} or TgN3^{R169C} mice. Further cell characterization showed that this increase was due to an enhanced survival of BrdU+/S100β+ cells ($F(4,60) = 6.037$, $p < 0.001$; post-hoc: STD vs. RUN, $p < 0.001$) (Fig. 2c) and particularly of BrdU+/NeuN+ cells ($F(4,60) = 4.147$, $p < 0.01$; post-hoc: STD vs. RUN and ENR, $p < 0.001$) (Fig. 2e).
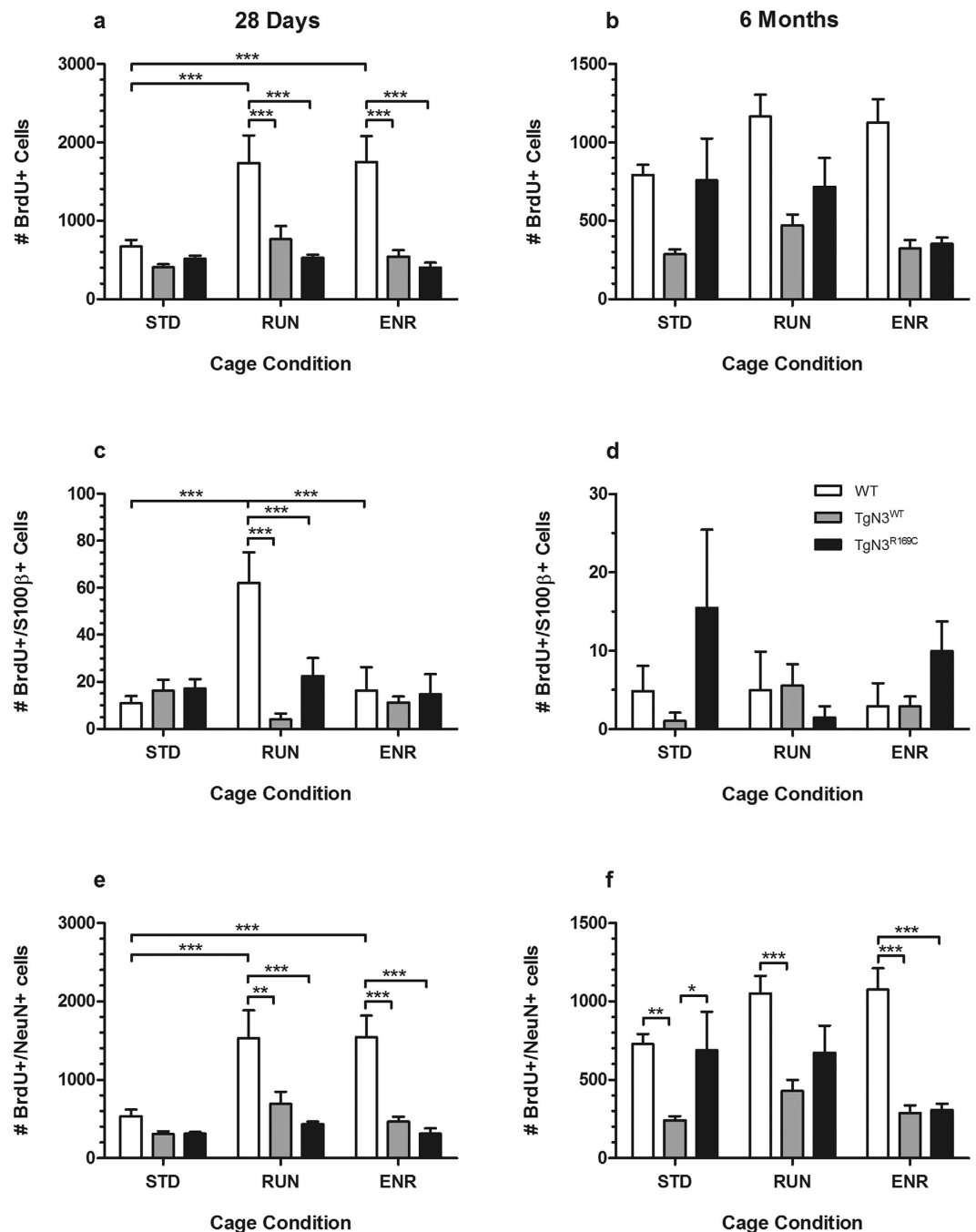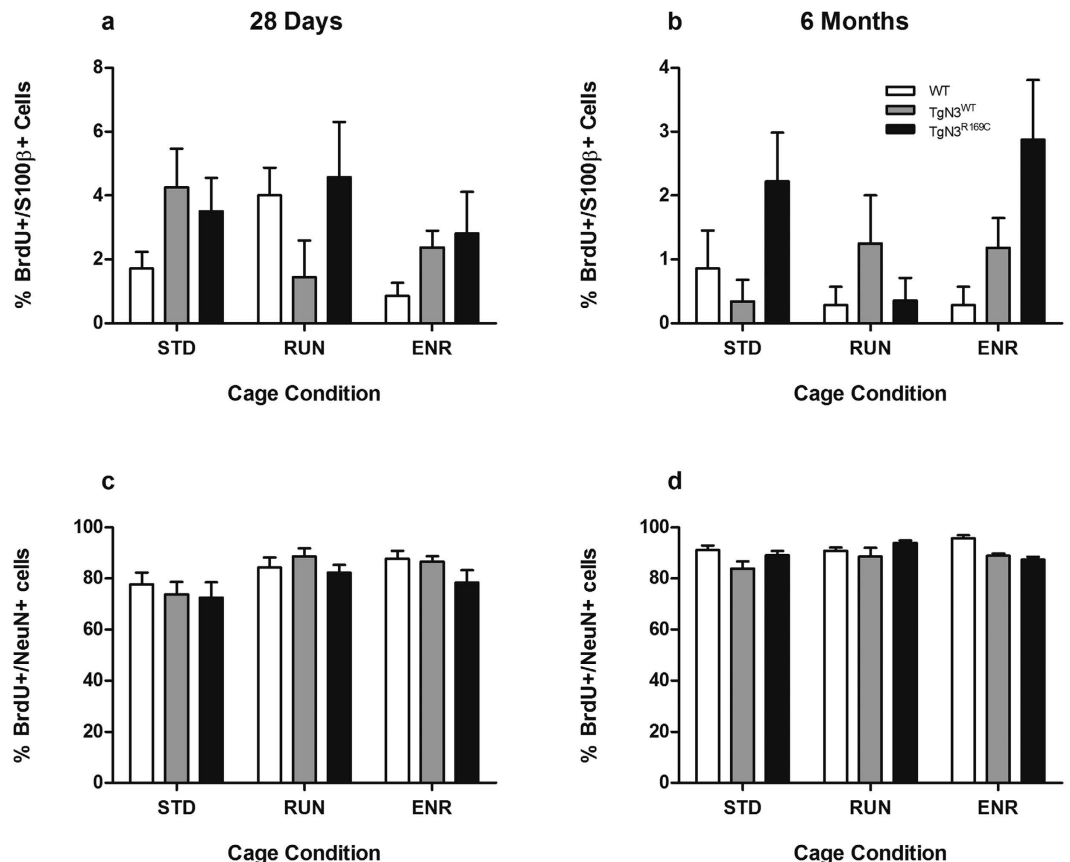
Figure 2. Results of the histological analysis of adult hippocampal neurogenesis in brain sections from WT, TgN3[WT] and TgN3[R169C] mice after 28 days (**a**,**c** and **e**) or 6 months (**b**,**d** and **f**) under standard (STD), running wheel (RUN) or environmentally enriched (ENR) cage conditions. The absolute number of BrdU+ (**a** and **b**), BrdU+/S100β+ (**c** and **d**) and BrdU+/NeuN+ cells (**e** and **f**) was quantified to determine the survival rate of proliferating cells, new astrocytic and new neuronal cells. New neuron survival is reduced in older (**f**) but not younger TgN3[WT] mice (**e**). Neurogenic stimulation by RUN or ENR failed in both TgN3[WT] and TgN3[R169C] independent of the duration (**e** and **f**). Data are expressed as mean ± S.E.M. *p < 0.05, **p < 0.01, ***p < 0.001.

No such increase of (neuronal) cell numbers was found after 6 months of RUN or ENR (BrdU+ cells: $F_{(4,53)} = 2.108$, $p > 0.05$; BrdU+/NeuN+ cells: $F_{(4,53)} = 2.415$, $p > 0.05$) either in WT or transgenic mice (STD vs. RUN or ENR: $p > 0.05$).

Representative microscope images of the BrdU staining are given in Fig. 5, demonstrating that WT mice display more BrdU+ cells after 28 days of RUN (Fig. 5d) and ENR (Fig. 5g) compared to STD (Fig. 5a). Figure 5 also shows that RUN and ENR did not stimulate BrdU+ cell survival in TgN3[WT] (Fig. 5b,e and h) or TgN3[R169C] mice (Fig. 5c,f and i).

Figure 3. Results of the histological analysis of adult hippocampal neurogenesis in brain sections from WT, TgN3[WT] and TgN3[R169C] mice after 28 days (**a** and **c**) or 6 months (**b** and **d**) under standard (STD), running wheel (RUN) or environmentally enriched (ENR) cage conditions. The percentage of BrdU+/S100β+ (**a** and **b**) and BrdU+/NeuN+ cells (**c** and **d**) of all BrdU+ cells was determined to assess effects on the differentiation of BrdU+ cells to astrocytes and neurons. The percentage of BrdU+/S100β+ cells in TgN3[R169C] is increased in older mice independent of RUN or ENR (**b**). Data are expressed as mean ± S.E.M.

Running wheel activity is reduced in CADASIL mice and age-dependently decreased in Notch3 overexpressing mice. During 28 days (Fig. 6a), TgN3[WT] mice showed increased running wheel activity per 24 h compared to WT and CADASIL mice ($F_{(2,543)} = 84.66$, $p < 0.001$; post-hoc: TgN3[WT] vs. WT and TgN3[R169C], $p < 0.001$). TgN3[R169C] mice in turn ran a shorter distance per 24 h than WT ($p < 0.001$).

During 6 months (Fig. 6b), in contrast, running wheel activity was reduced in transgenic mice ($F_{(2,1569)} = 229.7$, $p < 0.001$; post hoc: TgN3[WT] and TgN3[R169C] vs. WT, $p < 0.001$) with TgN3[R169C] mice running even less than TgN3[WT] mice ($p < 0.001$). Detailed analysis of running wheel activity over six months (Fig. 6c) revealed that the distance run per month decreased over time in TgN3[R169C] mice ($F_{(5,8)} = 8.121$, $p < 0.01$).

When considering just the first five days of RUN (Fig. 6d), which are most relevant for the stimulation of neural cell proliferation in the DG, WT and TgN3[WT] mice covered similar distances, while TgN3[R169C] mice showed significantly reduced physical activity per 24 h compared to WT and TgN3[WT] mice ($F_{(2,92)} = 22.34$, $p < 0.001$; post-hoc: $p < 0.001$).

Motor coordination on the Rotarod is impaired in both transgenic mouse lines. TgN3[WT] and TgN3[R169C] mice spent significantly less time on the rotating rod than WT mice ($F_{(2,16)} = 6.309$, $p < 0.01$; post-hoc: $p < 0.05$) (Fig. 6e). This indicates motor deficits in both transgenic mouse lines.

Discussion

The present study aimed to investigate whether adult hippocampal neurogenesis in CADASIL can be influenced in short- and long-term by physiological stimuli, which have been shown to robustly enhance it in healthy animals and neuropathological disease models[26–29]. We found that the long-term survival of new neurons was reduced in Notch3 overexpressing but not CADASIL mice under STD cage conditions compared to WT. Moreover, short- and long-term neurogenic stimulation by RUN or ENR apparently failed in both transgenic mouse lines.

The decreased neurogenesis in Notch3 overexpressing mice of the long-term group replicates the finding of our previous study in six-months-old TgN3[WT] mice[22]. The fact that the decreased neurogenesis already observed four weeks after BrdU cell labeling[22] is still evident after five more months, shows that this is really due to a suppression of cell proliferation by Notch3 overexpression, as suggested in our previous work, rather than an influence on cell
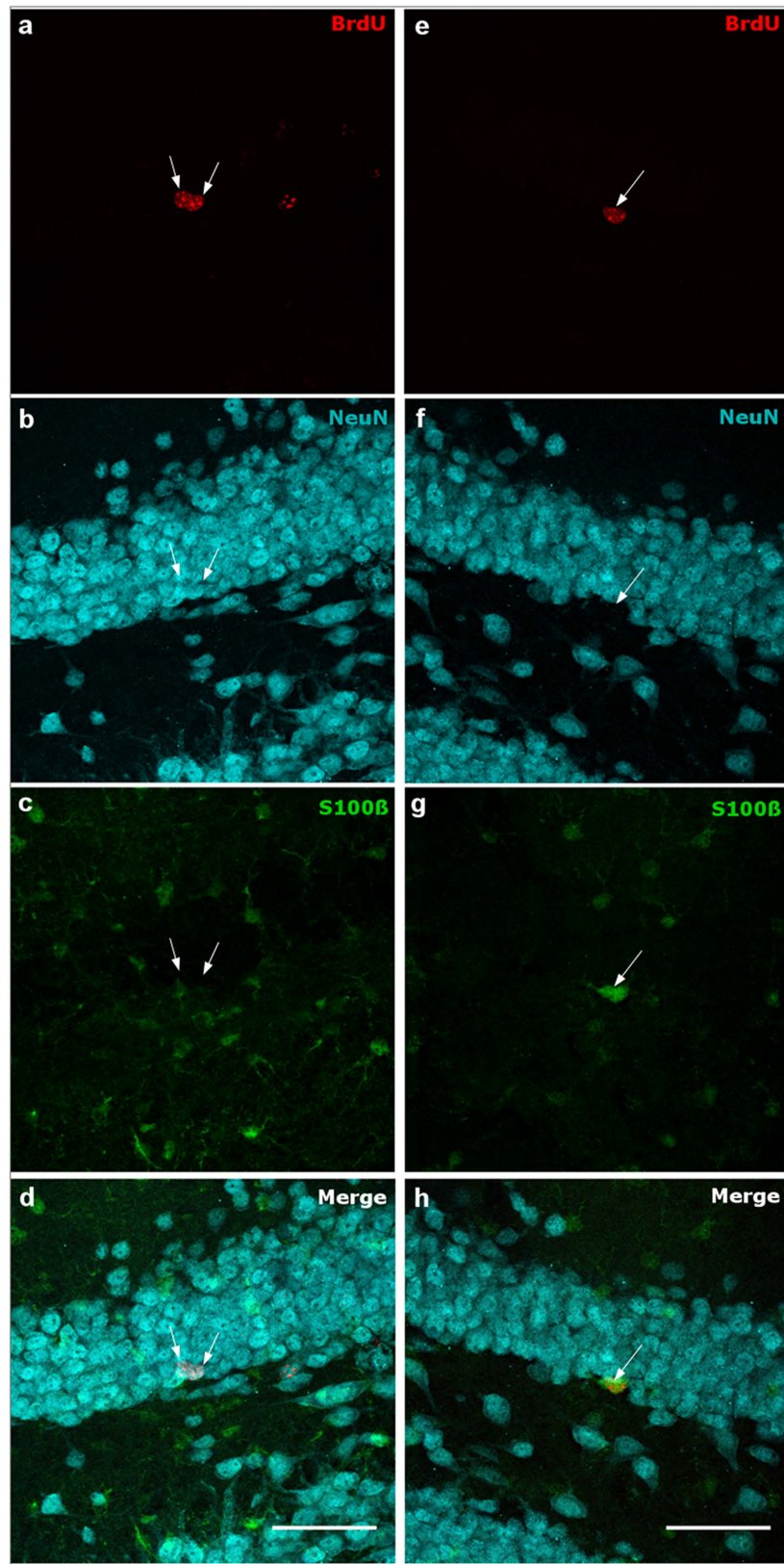
Figure 4. Representative confocal images of the triple fluorescent staining of the DG of two different mice (**a–d**): TgN3^{WT} ENR 6 months; (**e–h**) TgN3^{WT} STD 28 days). Arrows point to BrdU+ cell nuclei (red, **a** and **e**), NeuN+ cell nuclei (cyan, **b** and **f**), S100β+ cells (green, **c** and **g**), two BrdU+/NeuN+ cell nuclei (**d**) and a BrdU+/S100β+ cell (**h**). Scale bar = 50 μm.
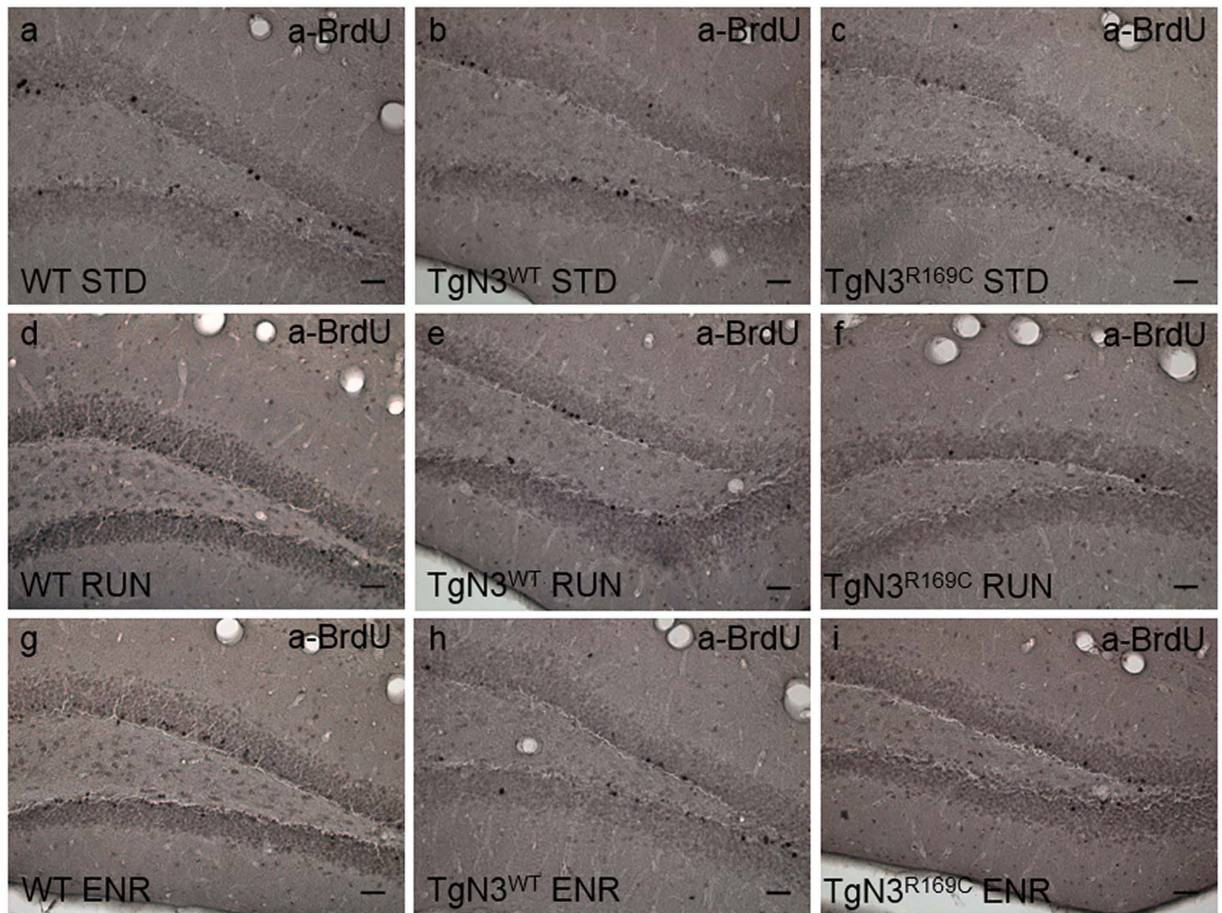
Figure 5. Representative light microscope images of the BrdU staining of the DG of each genotype after 28 days of STD (**a–c**), RUN (**d–f**) and ENR (**g–i**) cage conditions. They illustrate the increase in the number of BrdU-positive cells (black dots) in healthy WT animals after RUN (**d**) or ENR (**g**) and the missing stimulating effect on cell survival in Notch3 overexpressing (TgN3^{WT}) and CADASIL mice (TgN3^{R169C}). Scale bar = 100 μm.

survival. Notch3 and Notch1 are possibly co-expressed in proliferating hippocampal precursor cells[22]. Moreover, Notch1 has been shown to be essential for progenitor pool maintenance and regulation of proliferation[16,18,30]. Therefore, it can be assumed that the suppression of cell proliferation by Notch3 is usually counteracted by Notch1-activated cell proliferation leading to a balanced cell proliferation rate. Overexpression of Notch3 clearly shifts the balance towards a down-regulation of precursor cell proliferation. Surprisingly, neurogenesis is not suppressed in TgN3^{WT} mice under short-term STD conditions. This might indicate an age-dependency of Notch3-dependent suppression of hippocampal neurogenesis with a counteracting mechanism being effective in younger mice of the short-term group but being lost during ageing in the long-term group.

In CADASIL mice, neurogenesis is not decreased as in Notch3 overexpressing mice. However, more newly generated cells differentiate into astrocytic cells in the long-term than in WT mice. As astrocytes are critical for neurogenesis and the neuronal long-term survival[31], an increase in their portion here could represent a counteracting mechanism for a disturbed neurogenesis due to mutated and imbalanced Notch3. In support of this hypothesis, we also found an increased amount of astrocytic cells in WT animals induced by short-term RUN, which is similar to our previous findings showing different stimuli selectively affecting distinct subpopulation of newly generated hippocampal cells[32]. This may point towards the need for an intact microenvironment in the DG for a functional neurogenesis, as the generation of astrocytes is enhanced by RUN in parallel to neurogenesis.

Usually, RUN and ENR of short- or long-term durations are robust neurogenic stimulants in healthy or aged animals[33,34] and in various rodent models of neuropathological diseases such as Alzheimer's[29] and Parkinson's disease[26]. Here, RUN and ENR cage conditions increased hippocampal neurogenesis in healthy WT mice as expected. Although Notch3 overexpressing mice of the short-term group ran more in the running wheel than WT mice, despite a reduced motor coordination tested on the Rotarod, neurogenesis remains unaffected. This suggests that although neurogenesis is not yet reduced in younger TgN3^{WT} mice, it is already disturbed due to Notch3 overexpression as it could not be stimulated by RUN and ENR. In support of this, we have demonstrated in our previous work using a KCl-activation neurosphere assay that the proliferative activity of neural precursor cells was potentially reduced by Notch3 overexpression[22]. This might have prevented the activation by RUN or ENR. In contrast to the present results, Ables and colleagues[35] have been able to restore neurogenesis by RUN in a Notch1 knock-out mouse. Knock-out of Notch1 specifically diminished the undifferentiated cell pool in the SGZ
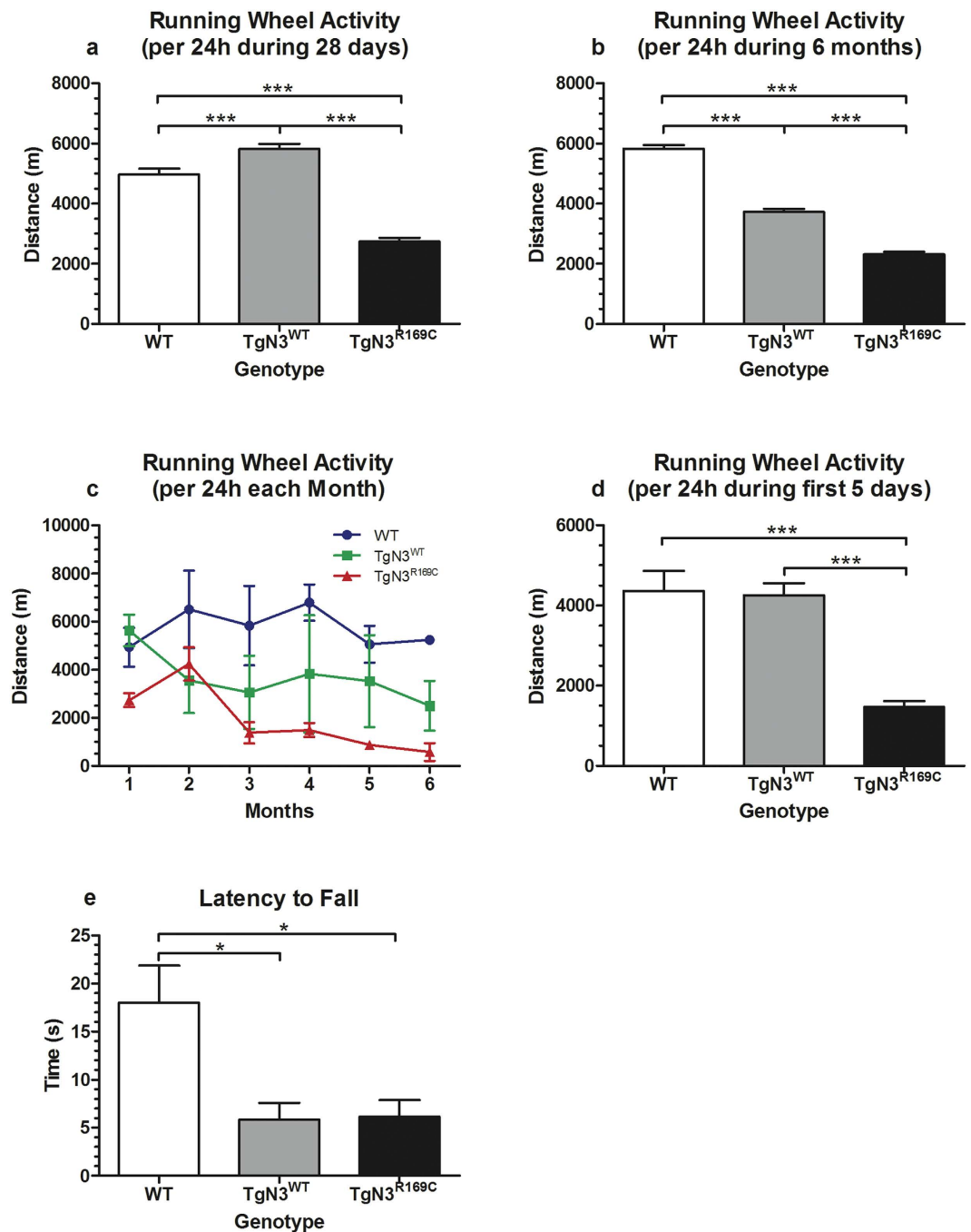
Figure 6. Effects of Notch3 overexpression (TgN3[WT]) and CADASIL (TgN3[R169C]) on physical activity per 24 h during 28 days (**a**), six months (**b** and **c**), during the first five days (**d**) under running wheel cage condition (RUN) and on Rotarod performance in transgenic mice corresponding to the 28 days group (**e**). Running wheel activity is reduced in TgN3[R169C] mice and duration-dependently decreased in TgN3[WT] mice (**a**–**d**). Motor coordination on the Rotarod is impaired in both transgenic mouse lines (**e**). Results of pairwise comparisons following a significant one-way ANOVA are displayed in the graphs. Data are expressed as mean ± S.E.M. *$p < 0.05$, ***$p < 0.001$.

causing a decreased neurogenesis. RUN rescued the number of differentiated but not undifferentiated cells, indicating that this neurogenesis stimulation might not be mediated by Notch1. To clarify, if Notch3 may be involved instead, as suggested by the present results, a similar knock-out model but for Notch3 or a Notch3 antagonist[36] could be used in follow-up studies.

In CADASIL mice, hippocampal neurogenesis was similarly not increased by RUN or ENR. In contrast to Notch3 overexpressing mice, CADASIL mice showed reduced physical activity in the running wheels throughout both durations. Motor coordination on the Rotarod was also impaired. This might be interpreted as the level of physical activity in RUN, and probably also in ENR, being insufficient to stimulate neurogenesis under this

neuropathological condition. However, running wheel activity of less than 2000 m covered distance per during 6 months has been shown to enhance neurogenesis[33]. In the present study, CADASIL mice ran mostly more than 2000 m per 24 h. Therefore, we suggest that the overexpression of mutated Notch3 disturbed the micromilieu of hippocampal precursor cells, which may have prevented these cells from reacting to RUN or ENR. This implies that not only functional Notch3 is crucial for the regulation of hippocampal neurogenesis but also its available amount in precursor cells itself and in the vascular neurogenic niche. This is of particular importance from a therapeutic point of view as it suggests that in CADASIL mutated Notch3 not only needs to be replaced but also the balance needs to be maintained.

Similar to CADASIL mice, Notch3 overexpressing mice also showed reduced physical activity (>2000 m distance covered) in the long-term and no stimulation of neurogenesis by RUN or ENR. But as they ran even more than WT mice in the short-term with still no change in neurogenesis levels, physical activity may not function as an adequate supportive therapy unless the amount of (functional) Notch3 is regulated at the same time. In ENR, however, physical activity is only one stimulation aside from visual, social and olfactory interaction with numerous other mice in a diversified equipped large cage. As the neurogenic stimulation by ENR was impaired to the same extent as by RUN, other functions than solely physical fitness could have been affected by mutated Notch3. Possible candidates are motivation, curiosity or anxiety, all of which might have been reduced in the transgenic mice, thus preventing the full experience of and benefit from ENR. This needs to be further investigated in these transgenic mouse lines.

In summary, we found that adult hippocampal neurogenesis *per se* is not altered in mice of the short-term group overexpressing wild type Notch3 or Notch3 with a CADASIL mutation. However, neurogenesis could not be stimulated by RUN or ENR of either duration, which may indicate a disturbed neurogenic process that is not reflected on the basal neurogenesis level. Considering this can be observed while no deficits in microcirculation or the vascular network have been reported[22,25], it suggests an additional independent role of Notch3 in hippocampal function. We conclude that cell intrinsic deficits in Notch3 signaling contributing to changes in adult hippocampal neurogenesis by changing the micromilieu is one vascular-independent mechanism in CADASIL patients, which might be a supporting factor for the development of cognitive deficits.

Methods

Animals. Two different transgenic mouse lines were used in this experiment. TgN3[R169C] mice carry the R169C point mutation at exon 4 of the *notch3* gene that causes cardinal pathological features of CADASIL[25]. TgN3[WT] mice express wild type Notch3[25]. Both transgenic lines show a 4-fold overexpression of either the mutated or the wild type Notch3 transcript and protein[25]. The FVB/N background strain served as control. FVB/N mice were obtained from Janvier Labs (Le Genest-Saint-Isle, France). Transgenic mice were bred in the Research Institutes for Experimental Medicine of the Charité Berlin (FEM). All experiments were approved by the local animal ethics committee (Landesamt für Gesundheit und Soziales, Berlin) and were carried out in accordance with the European Communities Council Directive of 22 September 2010 (10/63/EU). The genotype was confirmed by PCR following tail biopsies (Primers: Notch3 forward: 5′ TTC AGTGGTGGCGGGCGTC 3′; Notch3 reverse: 5′ GCCTACAGGTGCCACCATTA CGGC 3′; Vector forward: 5′ AACAGGAAGAATCGCAACGTTAAT 3′; Vector reverse: 5′ AATGCA GCGA TCAACGCCTTCTC 3′). To minimalize stress and conflicts in the experimental groups, only females were included in the experiments. Water and rodent lab chow were provided *ad libitum* and a constant twelve hours light/dark cycle was applied.

Experimental design. 131 eight to twelve week-old female FVB/N (WT), TgN3[R169C] and TgN3[WT] mice were each separated into three different cage conditions (Fig. 1). Mice maintained under standard conditions (STD) were housed in conventional cages (Makrolon cages, 0.27 m × 0.15 m × 0.42 m) in groups of two to five animals per cage. Mice kept in an enriched environment (ENR) were housed in groups of five to ten animals in larger cages (0.74 m × 0.3 m × 0.74 m), containing multiple plastic tubes, which varied in size and shape and were frequently rearranged, a cardbox house and a plastic house. In the third cage condition (RUN) mice were maintained in conventional cages in groups of two animals and provided with a running wheel (Tecniplast, Italy). Wheel turns were automatically recorded by LCD counters to monitor running wheel activity. Animals were kept in their specific cage condition either for a short (28 days) or a long (6 months) duration (Fig. 1). At the beginning of exposure to their specific cage condition, mice received three intraperitoneal (i.p.) injections of the mitotic marker Bromodeoxyuridine (BrdU, Sigma–Aldrich, Steinheim, Germany; 50 mg/kg in 0.9% NaCl) separated by an interval of 4 hours to label proliferating cells (Kuhn and Cooper-Kuhn, 2007) for the evaluation of their short- and long-term survival under the influence of wild type and mutated NOTCH3 overexpression as well as RUN and ENR.

A separate set of 20 eight to twelve week-old FVB/N, TgN3[R169C] and TgN3[WT] mice was exposed to the STD cage condition for 28 days and then tested on the Rotarod to assess motor coordination skills (Fig. 1)[37].

Rotarod. To test aspects of motor coordination, animals had to complete three consecutive trials on one day on the Rotarod (Columbus instruments, Columbus, OH, USA). The Rotarod consists of an elevated rod with modifiable rotating speed. Each mouse was placed on the rotating rod at a start speed of 5 rpm. When the animal found balance, the trial was started and the rod accelerated with a defined speed to a maximum of 65 rpm. The duration the animal could hold itself on the rotating rod was recorded automatically.

Perfusion and Tissue Processing. All animals were killed at the end of the experiment. First, the mice were deeply anesthetized with Ketamine/Xylazine (10% Ketamine hydrochloride, WDT; 2% Rompun, Provet AG; i.p. injection) and then transcardially perfused using 0.1 M phosphate buffered saline (PBS) followed by 4% paraformaldehyde in PBS. Brains were removed and post-fixed overnight in PFA at 4 °C and afterwards transferred

into 30% sucrose for 48 h for dehydration. Brains were then frozen in 2-methyl butane cooled with liquid nitrogen, and cut into 40 μm thick coronal sections (Bregma −0.22 mm to −3.80) using a cryostat (Leica CM 1850 UV).

Immunohistochemistry and immunofluorescence. Adult hippocampal neurogenesis was evaluated by quantifying the number of proliferating cells, which were characterized by the incorporation of BrdU. Therefore, a one-in-six series of free-floating brain sections of each animal was pretreated with H_2O_2 and HCl and then incubated with a primary anti-rat BrdU antibody (AbD serotec, 1:500) overnight at 4 °C. The next day, the sections were incubated with a biotinylated secondary antibody (Dianova, 1:125), followed by streptavidin peroxidase complex (Vectastain Elite ABC Kit, Vector Laboratories). Antibodies were visualized by diamoniobenzidine (DAB)-nickel staining, after which the brain sections were mounted on microscope slides and coverslipped.

For a more detailed investigation of neuronal and astrocytic cell types, a triple fluorescent staining against BrdU, the specific endogenous marker for Neuronal Nuclei (NeuN) and the specific marker for mature astrocytes S100β was performed. Therefore, a one-in-six series of free-floating brain sections of each animal was pretreated with HCl, followed by an overnight incubation at 4 °C with primary rat anti-BrdU antibody (AbD serotec, 1:500), mouse anti-NeuN (Millipore, 1:1000) and rabbit anti-S100β (Abcam, 1:150). The next day, sections were incubated with fluorescent secondary antibodies RhodamineX (Dianova, anti-rat, 1:250), Alexa 647 (Dianova, anti-mouse, 1:300) and Alexa 488 (Invitrogen, anti-rabbit, 1:1000) for four hours. Finally, brain sections were mounted on microscope slides and coverslipped.

Cell Quantification and image processing. For every animal, BrdU-positive (BrdU+) cells in the DAB staining were counted in nine sections containing the dentate gyrus (DG) with the SGZ, using a light microscope (Axioskop HB50/AC, Zeiss, Germany) and the 40× objective. Representative images of BrdU+ cells in the DG were taken using the 20× objective (Leica DMI 3000 B, bright field) and are shown in Fig. 5(a–i).

To detect fluorescently co-labeled BrdU/NeuN-positive (BrdU+/NeuN+) and BrdU/S100β-positive (BrdU+/S100β+) cells, 50 BrdU+ cells spread across the rostrocaudal extent of the DG were sequentially scanned (z-stacks) using a confocal microscope (Leica DM 2500). The obtained ratio was used to determine the absolute cell number. Representative confocal images of the triple fluorescent staining are shown in Fig. 4(a–h). The confocal images were taken using the 40x oil immersion objective. To get a whole image of the examined cells, 19 sequentially taken images were z-stacked. The distance between the images was 0.34 μm. Fiji for Windows 32 was used to adjust brightness and contrast.

Statistical analysis. The data sets of the short- and long-term group were graphically presented using GraphPad Prism 5 and separately analyzed using IBM SPSS Statistics 23. A two-way ANOVA was applied to analyze the effects of the investigated factors genotype and cage condition and their interaction on the numbers and percentages of BrdU+, BrdU+/NeuN+ and BrdU+/S100β+ cells. Running wheel activity during the short-term (28 days) and long-term (6 months) exercise intervention and Rotarod performance were analyzed by a one-way ANOVA. In case of a significant ANOVA, pairwise comparison using the Bonferroni post-hoc test was performed. The level of significance was set at $p \leq 0.05$.

References

1. Joutel, A. *et al.* Notch3 mutations in CADASIL, a hereditary adult-onset condition causing stroke and dementia. *Nature* **383,** 707–710 (1996).
2. Dichgans, M. Genetics of ischaemic stroke. *Lancet Neurol* **6,** 149–161 (2007).
3. Chabriat, H., Joutel, A., Dichgans, M., Tournier-Lasserve, E. & Bousser, M. G. Cadasil. *Lancet Neurol.* **8,** 643–653 (2009).
4. Joutel, A. *et al.* The ectodomain of the Notch3 receptor accumulates within the cerebrovasculature of CADASIL patients. *J. Clin. Invest.* **105,** 597–605 (2000).
5. Domenga, V. *et al.* Notch3 is required for arterial identity and maturation of vascular smooth muscle cells. *Genes Dev.* **18,** 2730–2735 (2004).
6. Craggs, L. J. *et al.* White matter pathology and disconnection in the frontal lobe in cerebral autosomal dominant arteriopathy with subcortical infarcts and leukoencephalopathy (CADASIL). *Neuropathol. Appl. Neurobiol.* **40,** 591–602 (2014).
7. Duering, M. *et al.* Strategic role of frontal white matter tracts in vascular cognitive impairment: a voxel-based lesion-symptom mapping study in CADASIL. *Brain* **134,** 2366–2375 (2011).
8. Taillia, H. *et al.* Cognitive alterations in non-demented CADASIL patients. *Cerebrovasc. Dis.* **8,** 97–101 (1998).
9. Amberla, K. *et al.* Insidious cognitive decline in CADASIL. *Stroke* **35,** 1598–1602 (2004).
10. Irvin, D. K., Zurcher, S. D., Nguyen, T., Weinmaster, G. & Kornblum, H. I. Expression patterns of Notch1, Notch2, and Notch3 suggest multiple functional roles for the Notch-DSL signaling system during brain development. *J. Comp. Neurol.* **436,** 167–181 (2001).
11. Van Praag, H. *et al.* Functional neurogenesis in the adult hippocampus. *Nature* **415,** 1030–1034 (2002).
12. Kempermann, G., Jessberger, S., Steiner, B. & Kronenberg, G. Milestones of neuronal development in the adult hippocampus. *Trends Neurosci.* **27,** 447–452 (2004).
13. Garthe, A., Behr, J. & Kempermann, G. Adult-generated hippocampal neurons allow the flexible use of spatially precise learning strategies. *PLoS ONE* **4,** e5464 (2009).
14. Kempermann, G. New neurons for 'survival of the fittest'. *Nat. Rev. Neurosci.* **13,** 727–736 (2012).
15. Spalding, K. L. *et al.* Dynamics of hippocampal neurogenesis in adult humans. *Cell* **153,** 1219–1227 (2013).
16. Breunig, J. J., Silbereis, J., Vaccarino, F. M., Sestan, N. & Rakic, P. Notch regulates cell fate and dendrite morphology of newborn neurons in the postnatal dentate gyrus. *Proc. Natl. Acad. Sci. USA* **104,** 20558–20563 (2007).
17. Hellstrom, M., Phng, L. K. & Gerhardt, H. VEGF and Notch signaling: the yin and yang of angiogenic sprouting. *Cell. Adhes. Migr.* **1,** 133–136 (2007).
18. Lugert, S. *et al.* Quiescent and active hippocampal neural stem cells with distinct morphologies respond selectively to physiological and pathological stimuli and aging. *Cell Stem Cell* **6,** 445–456 (2010).
19. Palmer, T. D., Willhoite, A. R. & Gage, F. H. Vascular niche for adult hippocampal neurogenesis. *J. Comp. Neurol.* **425,** 479–494 (2000).

20. Chabriat, H. *et al.* Cerebral hemodynamics in CADASIL before and after acetazolamide challenge assessed with MRI bolus tracking. *Stroke* **31,** 1904–1912 (2000).
21. Miao, Q. *et al.* Fibrosis and stenosis of the long penetrating cerebral arteries: the cause of the white matter pathology in cerebral autosomal dominant arteriopathy with subcortical infarcts and leukoencephaolopathy. *Brain Pathol.* **14,** 358–364 (2004).
22. Ehret, F. *et al.* Mouse model of CADASIL reveals novel insights into Notch3 function in adult hippocampal neurogenesis. *Neurobiol. Dis.* **75,** 131–141 (2015).
23. Van Praag, H., Kempermann, G. & Gage, F. H. Running increases cell proliferation and neurogenesis in the adult mouse dentate gyrus. *Nat. Neurosci.* **2,** 266–270 (1999).
24. Kempermann, G., Kuhn, H. G. & Gage, F. H. More hippocampal neurons in adult mice living in an enriched environment. *Nature* **386,** 493–495 (1997).
25. Joutel, A. *et al.* Cerebrovascular dysfunction and microcirculation rarefaction precede white matter lesions in a mouse genetic model of cerebral ischemic small vessel disease. *J. Clin. Invest.* **120,** 433–445 (2010).
26. Klein, C. *et al.* Physical exercise counteracts MPTP-induced changes in neural precursor cell proliferation in the hippocampus and restores spatial learning but not memory performance in the water maze. *Behav. Brain Res.* **307,** 227–238 (2016a).
27. Klein, C. *et al.* Exercise prevents high-fat diet-induced impairment of flexible memory expression in the water maze and modulates adult hippocampal neurogenesis in mice. *Neurobiol. Learn. Mem.* **131,** 26–35 (2016b).
28. Iggena, D. *et al.* Only watching others making their experiences is insufficient to enhance adult neurogenesis and water maze performance in mice. *Sci. Rep.* **5,** 14141 (2015).
29. Wolf, S. A. *et al.* Cognitive and physical activity differently modulate disease progression in the amyloid precursor protein (APP)-23 model of Alzheimer's disease. *Biol. Psychiatry* **60,** 1314–1323 (2006).
30. Stump, G. *et al.* Notch1 and its ligands Delta-like and Jagged are expressed and active in distinct cell populations in the postnatal mouse brain. *Mech. Dev.* **114,** 153–159 (2002).
31. Seki, T. Microenvironmental elements supporting adult hippocampal neurogenesis. *Anat. Sci. Int.* **78,** 69–78 (2003).
32. Steiner, B. *et al.* Differential regulation of gliogenesis in the context of adult hippocampal neurogenesis in mice. *Glia* **46,** 41–52 (2004).
33. Kronenberg, G. *et al.* Physical exercise prevents age-related decline in precursor cell activity in the mouse dentate gyrus. *Neurobiol. Aging* **27,** 1505–1513 (2006).
34. Kempermann, G., Gast, D. & Gage, F. H. Neuroplasticity in old age: sustained fivefold induction of hippocampal neurogenesis by long-term environmental enrichment. *Ann. Neurol.* **52,** 135–143 (2002).
35. Ables, J. L. *et al.* Notch1 is required for maintenance of the reservoir of adult hippocampal stem cells. *J. Neurosci.* **30,** 10484–10492 (2010).
36. Yen, W.-C. *et al.* Targeting Notch signaling with a Notch2/Notch3 antagonist (Tarextumab) inhibits tumor growth and decreases tumor-initiating cell frequency. *Clin. Cancer Res.* **21,** 2084–2095 (2015).
37. Karl, T., Pabst, R. & von Hörsten, S. Behavioral phenotyping of mice in pharmacological and toxicological research. *Exp. Toxicol. Pathol.* **55,** 69–83 (2003).

Acknowledgements

Author Contributions

C.K., A.P. and T.M. performed the animal experiments including behavioral testing. S.S., F.E.K. and P.E. accomplished the histological stainings and cell quantifications. C.K. conducted the data-analysis. C.K. and S.S. wrote the manuscript. B.S. conceived and designed the study and wrote the manuscript.

Additional Information

Competing Interests: The authors declare no competing financial interests.

How to cite this article: Klein, C. *et al.* Stimulation of adult hippocampal neurogenesis by physical exercise and enriched environment is disturbed in a CADASIL mouse model. *Sci. Rep.* **7,** 45372; doi: 10.1038/srep45372 (2017).

Publisher's note: Springer Nature remains neutral with regard to jurisdictional claims in published maps and institutional affiliations.

Curriculum vitae

Mein Lebenslauf wird aus datenschutzrechtlichen Gründen in der elektronischen Version meiner Arbeit nicht veröffentlicht.

List of publications

Research Articles	Pfeffer, A., Munder T, Schreyer S, Klein C, Rasińska J, Winter Y, Steiner B. *Behavioral and psychological symptoms of dementia (BPSD) and impaired cognition reflect unsuccessful neuronal compensation in the pre-plaque stage and serve as early markers for Alzheimer's disease in the APP23 mouse model.* Behav Brain Res, 2018. 347: p. 300-313.
	Munder, T., Pfeffer A, Schreyer S, Guo J, Braun J, Sack I, Steiner B, Klein C. *MR elastography detection of early viscoelastic response of the murine hippocampus to amyloid β accumulation and neuronal cell loss due to Alzheimer's disease.* J Magn Reson Imaging, 2018. 47(1): p. 105-114.
	Klein, C, Schreyer S, Kohrs FE, Elhamoury P, Pfeffer A, Munder T, Steiner B. *Stimulation of adult hippocampal neurogenesis by physical exercise and enriched environment is disturbed in a CADASIL mouse model.* Sci Rep, 2017. **7**: p. 45372.
Conference Contributions (Poster Presentation)	Pfeffer A, Munder T, Schreyer S, Klein C, Winter Y, Steiner B. *Further characterization of the young APP23 mouse offers new chances for early AD screening and therapy.* 10th FENS Forum of Neuroscience, July 2016 (Copenhagen, Denmark).

Acknowledgements

My years as a PhD student would not have been possible and as successful and inspiring without